

APPLICATION OF REFLECTION AND REFRACTION
TO ESTIMATE RESIDUAL STATIC
CORRECTIONS CAUSED BY NEAR SURFACE
HETEROGENEITY IN SAUDI ARABIA

by

Tassier Al-Yacoub
September 1988

ProQuest Number: 10781178

All rights reserved

INFORMATION TO ALL USERS

The quality of this reproduction is dependent upon the quality of the copy submitted.

In the unlikely event that the author did not send a complete manuscript and there are missing pages, these will be noted. Also, if material had to be removed, a note will indicate the deletion.



ProQuest 10781178

Published by ProQuest LLC (2018). Copyright of the Dissertation is held by the Author.

All rights reserved.

This work is protected against unauthorized copying under Title 17, United States Code
Microform Edition © ProQuest LLC.

ProQuest LLC.
789 East Eisenhower Parkway
P.O. Box 1346
Ann Arbor, MI 48106 – 1346

ER-3574


ER-3574

An Engineering Report submitted to the Faculty and the Board of Trustees of the Colorado School of Mines in partial fulfillment of the requirements for the Degree of Master of Engineering (Geophysics).

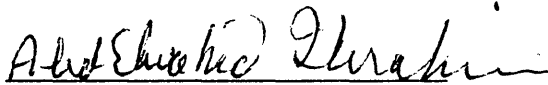
Golden, Colorado

Date 9/19/1988

Signed:



Taïsser Al-Yacoub

Approved:


Abdelwahid Ibrahim
Advisor

Golden, Colorado

Date 9/19/88


Phillip R. Romig, Jr.
Professor of Geophysics
and Head of Department
of Geophysics

ABSTRACT

The goal of this report is to explain the effectiveness of a software package developed by Western Geophysical in solving long wave length static problems on seismic data acquired in Saudi Arabia. Brute stack produces a poor image to subsurface structure because of lack of weathering thickness and velocity information. Automatic Reflection Program (MISER) proved incapable of solving the problem because the anomaly is larger than the cable length. The extended generalized reciprocal method is effective in estimating effects of near surface inhomogeneties resulting from long wave length static anomalies. The stack section is enhanced by applying reflection static after applying refraction static to remove the remaining short wave length static.

TABLE OF CONTENTS

ABSTRACT	1
1. INTRODUCTION	2
1.1 Purpose of Static Correction	2
1.2 Weathering Velocity and Its Effects	5
1.3 Data Description	8
2. FIELD STATIC CORRECTION	11
2.1 Field Static and Initial Stack	11
2.2 Results and Further Work	13
3. AUTOMATIC RESIDUAL STATIC CORRECTIONS (MISER)	18
3.1 Model and Assumption	18
3.2 Scheme of Decomposition	21
3.3 Residual Static Application	23
3.4 Results and Further Work	23
4. EXTENDED GENERALIZED RECIPROCAL METHOD (EGRM)	25
4.1 Introduction to the EGRM Theory	25
4.2 Application of EGRM Theory	26
4.2.1 Examine First Breaks	28
4.2.2 Picking the First Breaks	29
4.2.3 Refractor Velocity Calculation	33
4.2.4 Time-Depth Estimation	37
4.2.5 Refractor Elevation and Weathering Velocity Estimation	42
4.2.6 Static Computation	42
4.3 Results of EGRM Stack Section	46
5. APPLICATION OF MISER TO EGRM STACK-SECTION	51
6. CONCLUSIONS	53
REFERENCES	54

LIST OF FIGURES

FIGURE 1.	Static Effect on Deep Reflector	3
FIGURE 2.	Placing Shot and Receiver on a Datum Plane	4
FIGURE 3.	Surface Consistent Shot Static	6
FIGURE 4.	Surface Consistent Receiver Static	7
FIGURE 5.	Elevation Profile	9
FIGURE 6.	Field Static Parameters	12
FIGURE 7.	Processing Steps to Obtain Initial Stack Section	14
FIGURE 8.	Three Shot Records a Cable Length Apart	16
FIGURE 9.	Four Shot Records a Cable Length Apart	17
FIGURE 10.	Picking Travel Time Deviations From NMO-Corrected Gathers	19
FIGURE 11.	Surface Consistent Statics Model	20
FIGURE 12.	Processing Steps for a MISER Stack Section	24
FIGURE 13.	Refractor Theory Ray Path	27
FIGURE 14.	A Shot Record with L.M.O. Window	30
Figure 15.	The Same Shot After L.M.O. Correction	31
Figure 16.	Refractor Velocity Ray Path	34
FIGURE 17.	Velocity Analysis of Each Station	36

LIST OF FIGURES
(Continued)

FIGURE 18.	Refractor Velocity Profile for the Entire Line	38
FIGURE 19.	EGRM Time-Depth Ray Path	39
Figure 20.	Refractor Elevation Profile	43
FIGURE 21.	Weathering Velocity Profile for the Entire Line	44
FIGURE 22.	Shot Static Profile	47
FIGURE 23.	Receiver Static Profile	48
FIGURE 24.	Processing Steps for EGRM Stack Section	49
FIGURE 25.	Processing Steps for EGRM-MISER Stack Section	52

LIST OF PLATES

- Plate 1: Initial Stack - No Refraction
- Plate 2: MISER Applied to Initial Stack
- Plate 3: Seismic Data Coordinate Transform Display
- Plate 4:
 - 4.A Plot of Refracted Arrival Pick Time
 - 4.B EGRM Time-Depth Distribution
 - 4.C Iterative Shot Time-Depth Distribution
 - 4.D Iterative Receiver Time-Depth Distribution
- Plate 5:
 - 5.A Refractor and Weathering Velocity Profiles
 - 5.B Refractor Model for the Entire Line
 - 5.C Plot of Difference Between EGRM Statics and MISER Statics
 - 5.D Plot of Statics Computed from the Refractor Model and Final Datum of 1,800 ft and Replacement Velocity of 16,500 f/sec.
- Plate 6: EGRM Brute Stack Section
- Plate 7: MISER Applied to EGRM Stack Section

ACKNOWLEDGMENTS

I would like to express my gratitude to the Arabian American Oil Company (ARAMCO) for sponsoring and providing the data. I would also like to express my sincere thanks to my advisor, Dr. Ibrahim Abdelwahid, who has contributed generously during all stages of this research. I appreciate the help and guidance of Dr. Phillip R. Romig and Dr. Ronald Knoshaug, who served as members of my committee.

I wish to thank Dr. A. Fouda and Dr. M. I. Husseini from ARAMCO, Exploration Department, for suggesting a very interesting thesis topic and providing enthusiasm, support and advice.

I am indebted to the employees of the Western-Geophysical Company (Denver office) for their generous hospitality and allowing me to use their computer facilities. Special thanks go to Mr. Ben Quentana, Mr. Chuck Diggins, Mr. Charles Carvill, Mr. Dan Wisecup, Mr. Bruce Mootman; without their support and guidance, this thesis would not be possible.

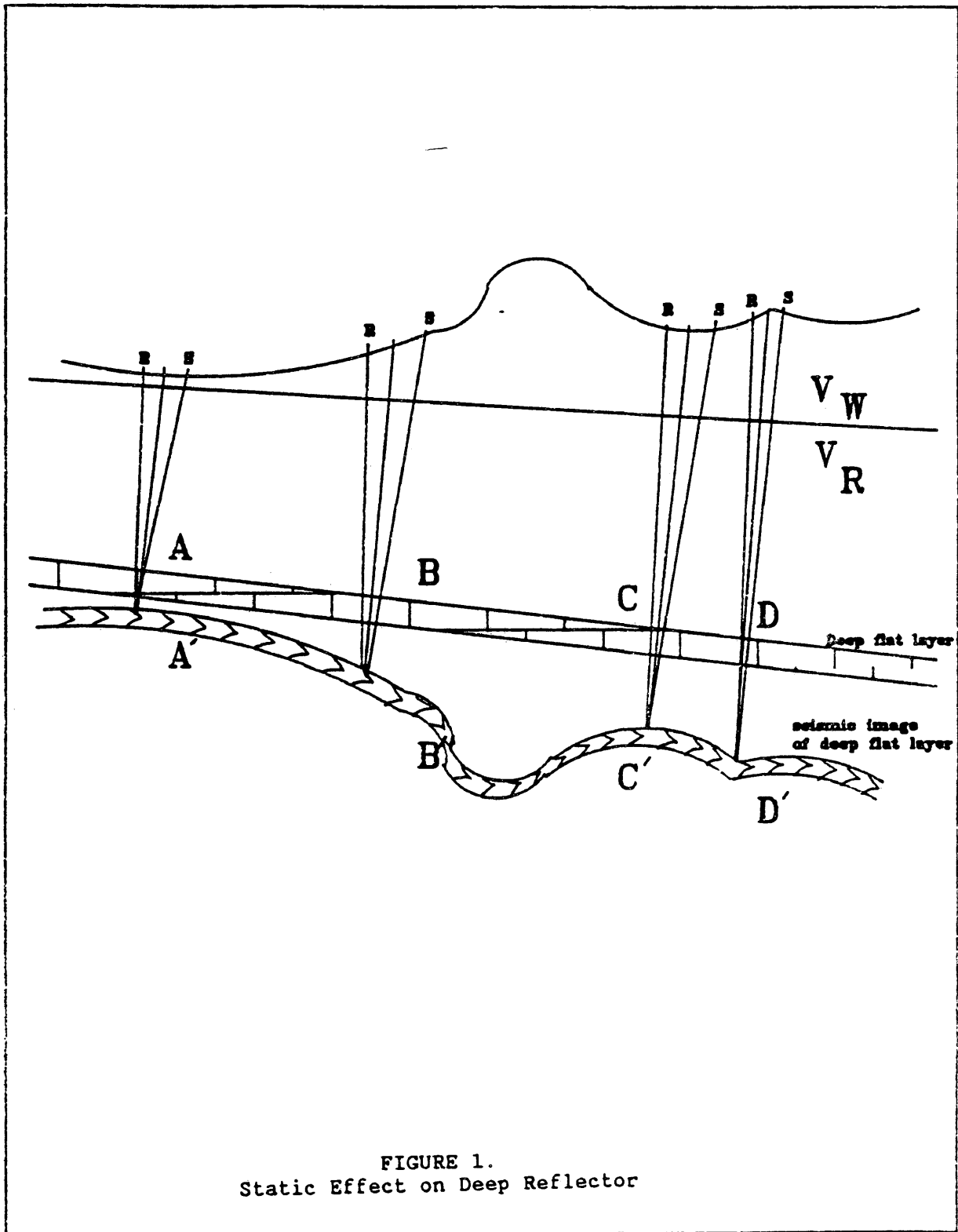
I extend my gratitude to my family--my mother, my brothers and my sisters for their prayers and encouragement. Last, but not least, a great full thanks and respect go to my wife, Ebtissam, who devoted all of her time as an excellent mother, taking care of our five children and acting as a wonderful teacher to them, teaching them the Arabic language, Islamic religion and arithmetics. Her efforts were instrumental for two of the children to pass the third grade.

1. INTRODUCTION

1.1 Purpose of Static Correction

The purpose of the static correction is to remove the effects of surface elevation changes and changes in the velocity of the weathered layer, and to relate the subsurface events to a datum elevation. This is necessary to eliminate the effect of low velocity, near surface material on the shape of a reflected event on a seismic section. A deep, flat reflector, for example, might apparently reflect the shape of the surface elevations if the static correction were not applied as in Figure 1.

The application of static corrections to data simulates the placing of both source and receiver on the datum at points vertically below (or above) their actual positions and where the weathered layer does not exist. Thus in Figure 2, the source static is the travel time from the source to a datum through the weathering and partly through the consolidated layer and the same definitions also applies to receiver static.



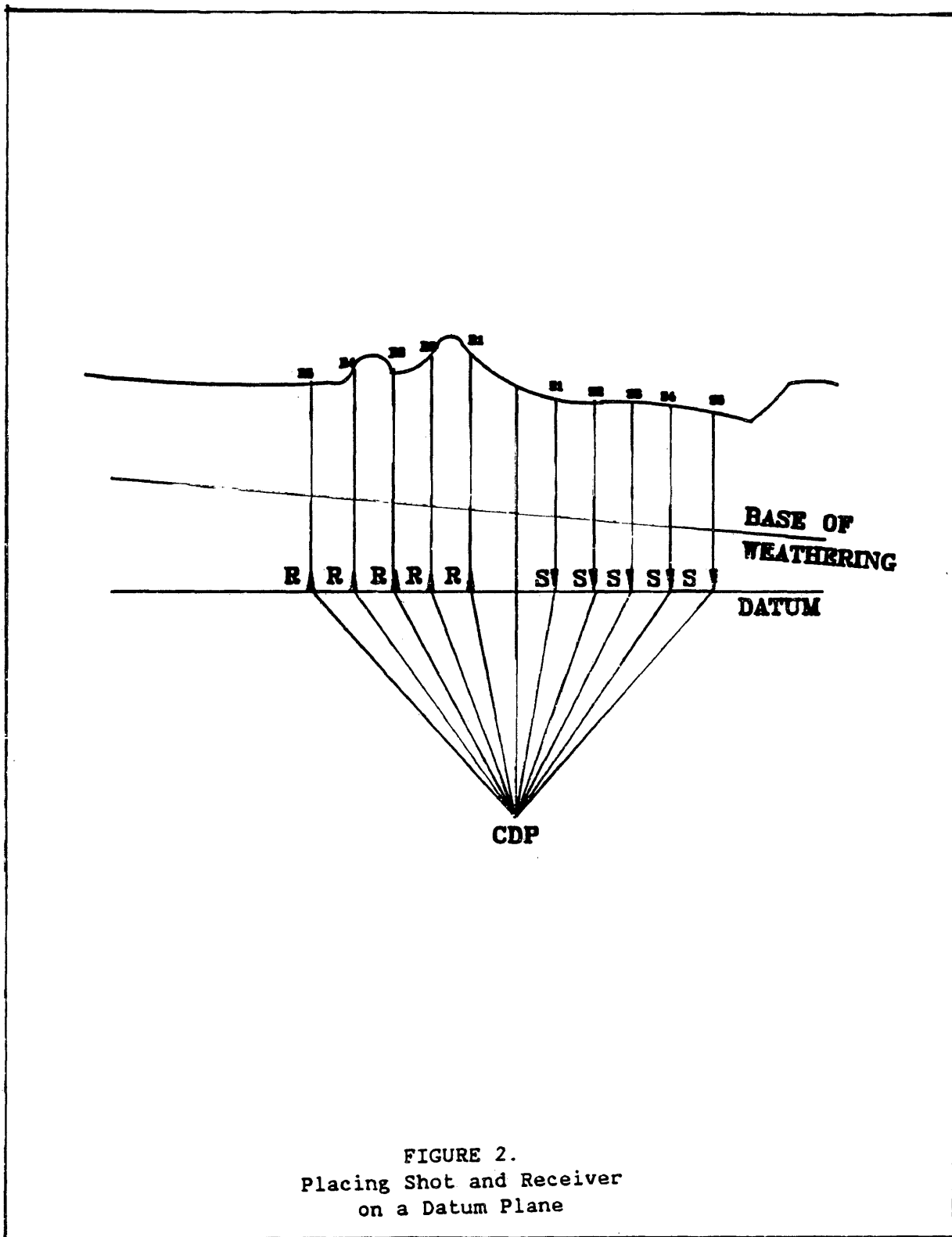
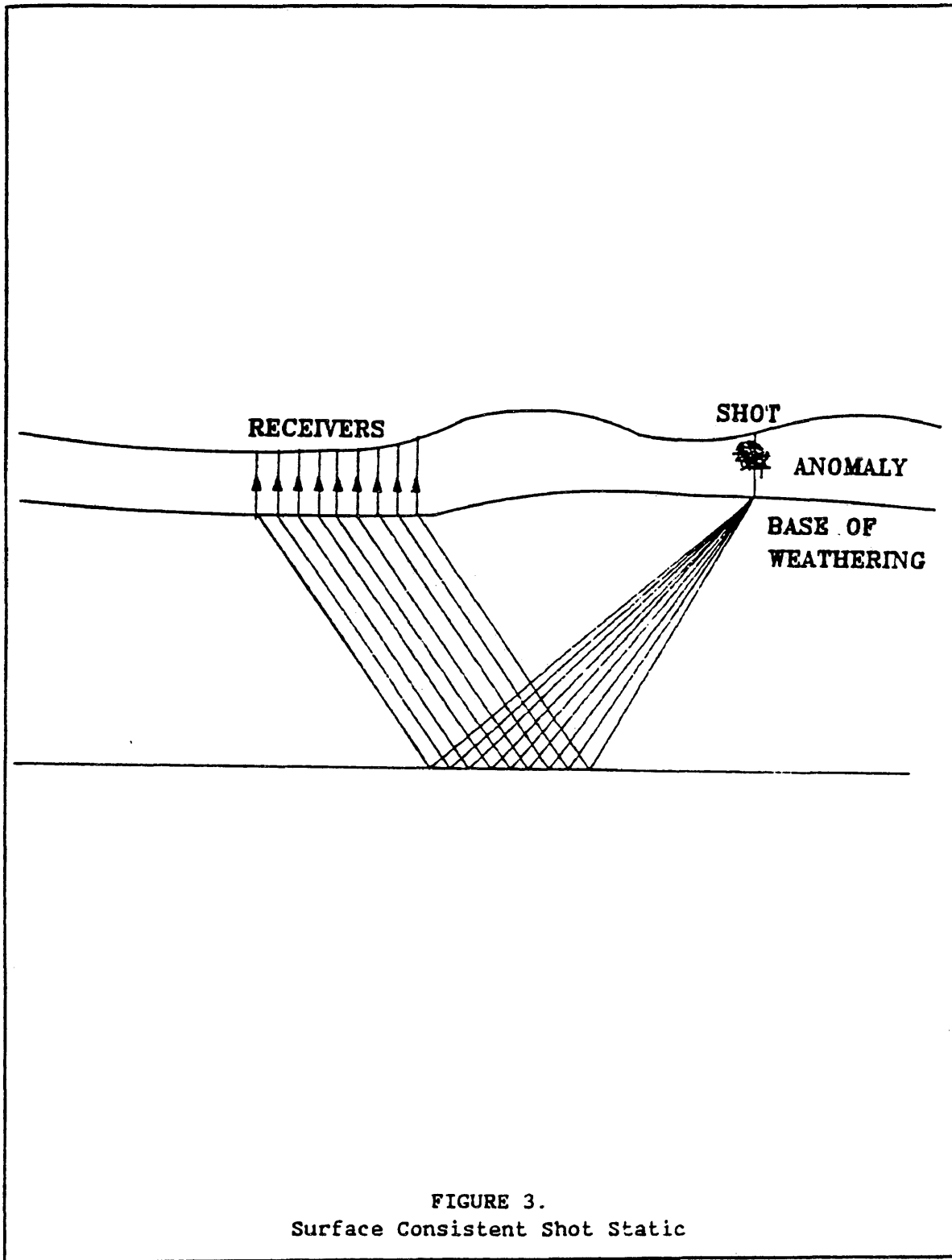


FIGURE 2.
Placing Shot and Receiver
on a Datum Plane

1.2 Weathering Velocity and Its Effects

The weathered layer is usually defined as the near surface unconsolidated layer. This layer is identified by low velocity of the order of 1800-6000 feet/sec. in Saudi Arabia. This layer's thickness usually varies with location; for example, the existence of an old river bed or sand dunes of different elevations may cause such variation. In this project, geological maps and well control was used to define the weathering layer and map its elevation and thickness at different points along the seismic line.

Lateral variation in the weathering layer could affect all records corresponding to one shot location if the velocity anomaly exists under that shot point as indicated in Figure 3. Also, many shot records could be affected partially by time shift deviations when velocity anomalies exist under these station locations; in other words, many shot records could be affected from that anomaly if the receiver of that record lies on that station as indicated in Figure 4. This is the basic assumption in static correction analysis defined as surface consistency assumption. This means that static shifts are time delays that solely depend on source or



ARTHUR LAKES LIBRARY
COLORADO SCHOOL of MINES
GOLDEN, COLORADO 80401

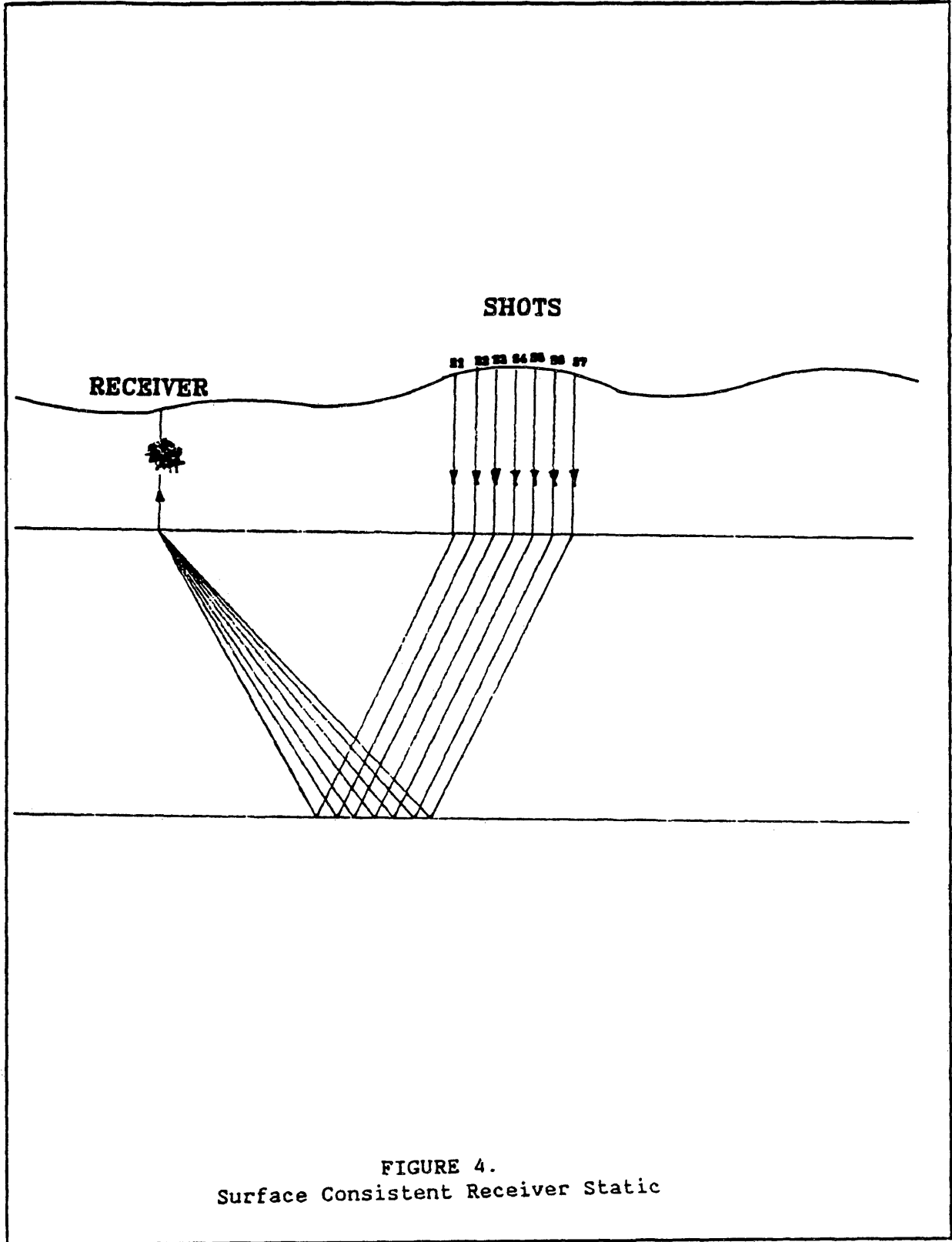


FIGURE 4.
Surface Consistent Receiver Static

receiver locations at the surface, not on the ray paths in the subsurface. This assumption is validated if all ray paths, regardless of source-receiver offset, are vertical in the near surface layering. Correct static corrections remove the effect of near surface inhomogeneous variations and allow referencing the seismic data to a uniform datum plane as indicated in Figure 2.

1.3 Data Description

The data on this project is a portion from an E-W seismic line in the Eastern Province of Saudi Arabia. This portion covers an area of approximately 31 km long (19.38 miles) and contains 1,299 source stations, starting with a Station #9477 on the East and ending with Station #10775 to the West. The source is vibroseis, off-end shooting with 240 traces, and a group interval of 24 meters. Figure 5 shows the elevation profile of this portion with station numbers on the x-axis and elevation in feet on the y-axis.

The geology of this area is mid-Cretaceous to upper Jurassic sediment. The layers dip to the east with 2° and are covered with a thick layer of sand and gravel between Stations 9477 and 9700. The area between stations

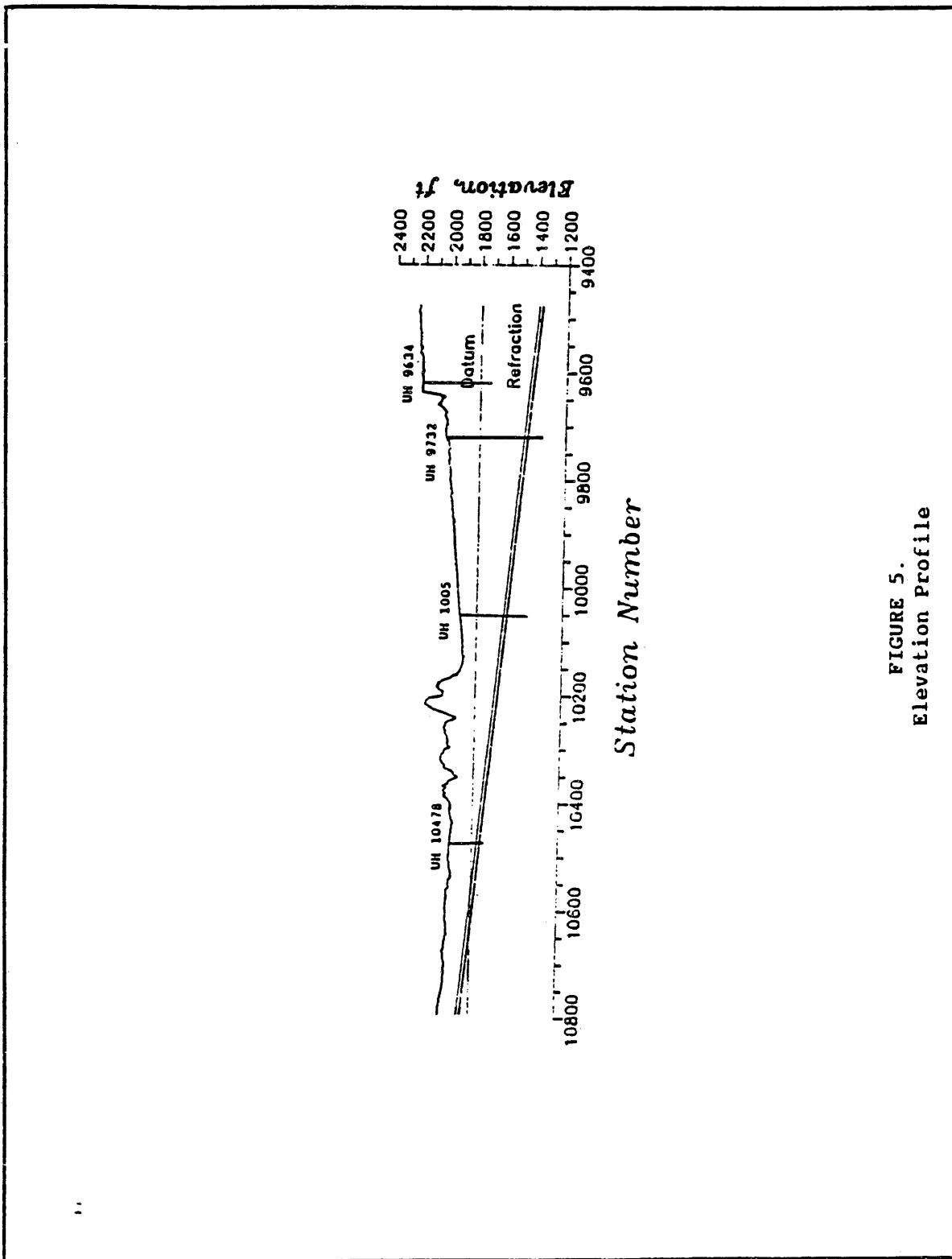


FIGURE 5.
Elevation Profile

8700-10400 is also covered with sand dunes of variable heights and medium thickness of sand between stations 10400-10755.

2. FIELD STATIC CORRECTION AND INITIAL STACK

2.1 Field Static

In this project, field static calculations are based on elevation values at the shot and receiver locations, and on assumed velocity. Since this line was an extension to an existing line in Saudi Arabia, the same processing parameters such as weathering velocity and datum elevation are applied in this study. A 5,500 ft/sec was chosen for weathering velocity and a datum of 1,800 feet was assumed in carrying out the field static correction. These values were based on uphole studies on other parts of the seismic line. Source and receiver field static were calculated as follows (Figure 6):

$$\text{Source Static} = \frac{ED-ES}{V_r}$$

$$\text{Receiver Static} = \frac{ED-ER}{V_r}$$

refer to Figure 6

ES = Source elevation (ft)

ER = Receiver elevation (ft)

ED = Datum elevation (ft)

V_r = Replacement velocity (ft/sec) (an estimate of
the average weathering velocity)

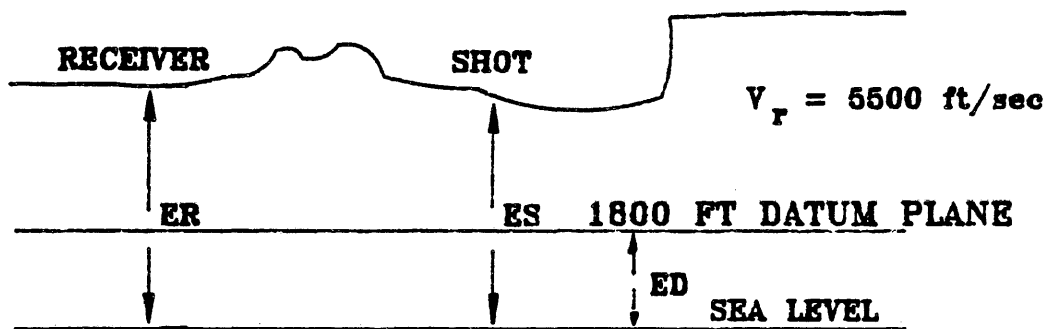


FIGURE 6.
Field Static Parameters

These shot and receiver statics are used in the processing sequence shown in Figure 7 to obtain the initial stack section (Plate 1).

2.2 Results and Further Work

The seismic section on Plate 1 represent initial stack section as a result of application of the field static. For analysis purposes, the seismic section on Plate #1 could be viewed horizontally in three parts, each part has many horizons. All the horizons in the first part are poorly imaged between Stations 9470-9900. This poor image is caused by the presence of very thick, low velocity material (sand and gravel). Uphole study at Station 9732 indicates presence of a filling of about 750 ft thick overlying a hard limestone layer. So this thick, low velocity material absorbs the energy and causes static problems for deep horizons. A shot record display in Figure 8 and Figure 9 also shows the distribution of a poor reflectivity between Stations 9470-9900.

The seismic section between Stations 9900-10400 has two shortcomings: The first is a distortion to the shallow data; the second is a time sag of about 170 ms affects events between .5 to 1.5 seconds. This time sag

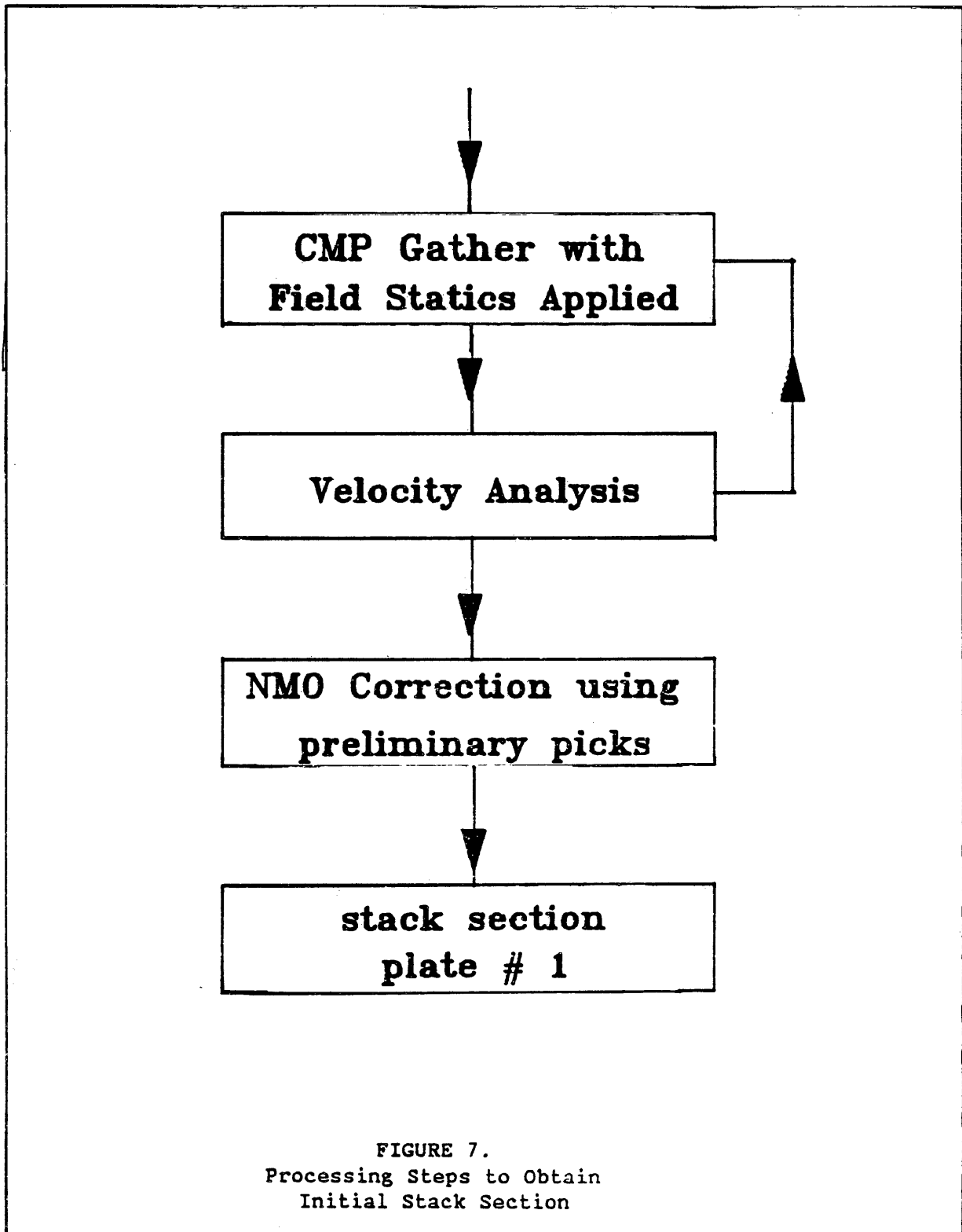


FIGURE 7.
Processing Steps to Obtain
Initial Stack Section

is caused by static problems related to sand dunes and inaccuracies in estimating the thickness and velocity of the weathering layer. Seismic traces between Station 9960 on Figure 8 and station 10440 on Figure 9 show the resulting distortion on the shot record data. Data quality is best in the seismic section between Station 10440-10775 because the weathering thickness is about 200 ft and the surface topography is smooth. A shot record in Figure 9 under Stations 10440, 10680, 10775 show an example of good data.

The four upholes in the area as indicated in Figure 5 show a high degree of variability in weathering velocities and depths to the subweathering zones. These facts indicate that the sag anomaly is caused by a low velocity fill zone and the existence of sand dunes to the west of the fill valley which has not been properly corrected for by the datum statics. Since the field statics and datum correction never totally compensate for the effects of near surface velocity variations. Automatic residual statics correction might be used to remove the near surface effects.

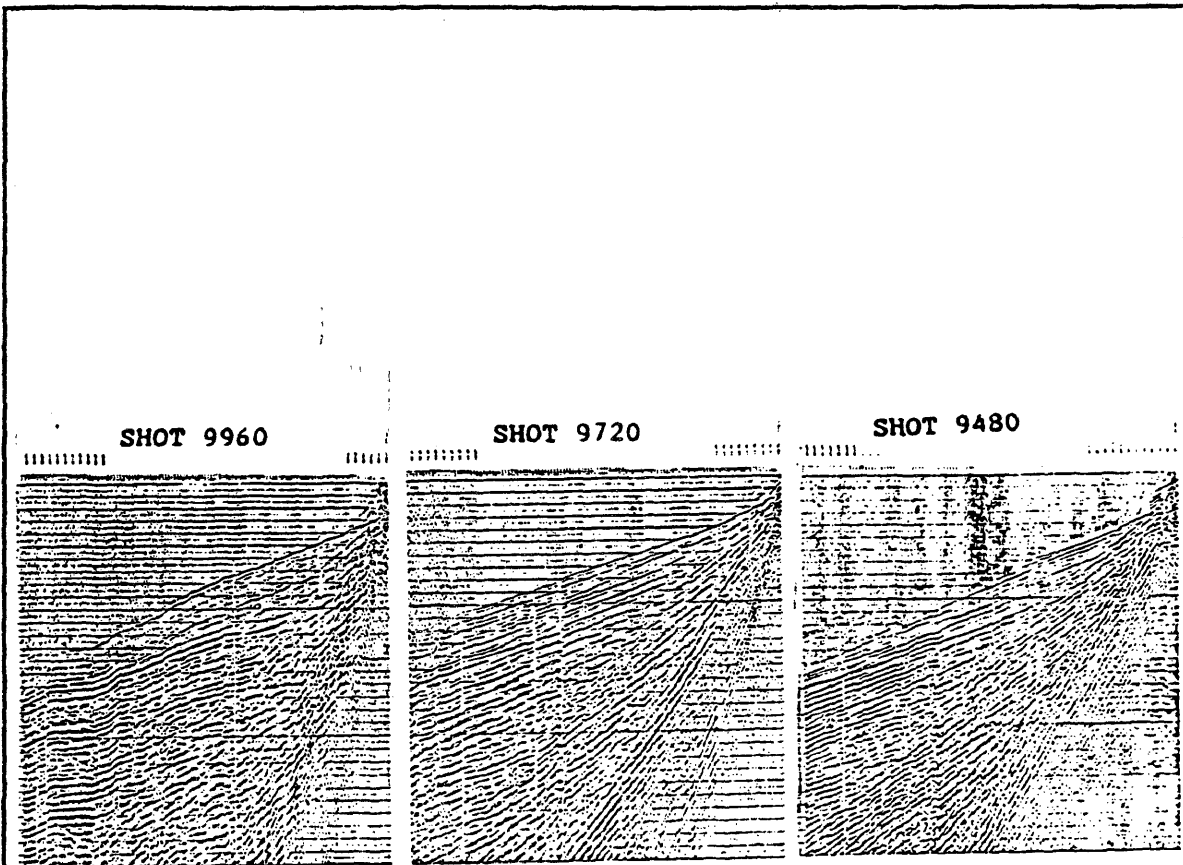


FIGURE 8.
Three Shot Records a Cable Length Apart

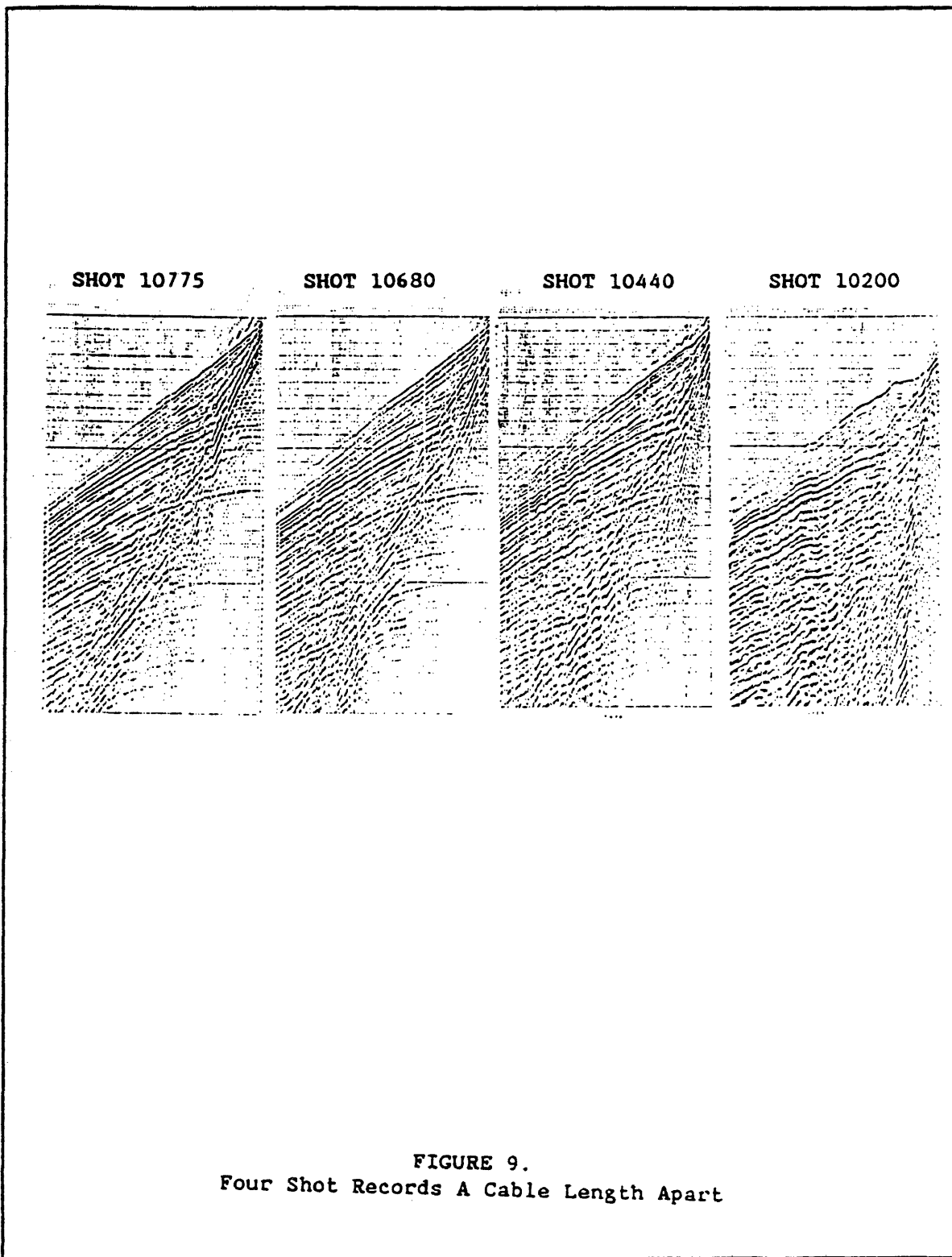


FIGURE 9.
Four Shot Records A Cable Length Apart

3. AUTOMATIC RESIDUAL STATIC CORRECTIONS (MISER)

3.1 Model and Assumption

Residual static deviation will introduce a misalignment of the waveforms across NMO corrected CMP gather (Figure 10). This results in a poor stack trace. To estimate the time shifts from the time of perfect alignment and correct for them automatically, a model is needed (Figure 11). Taner et al. (1974) suggested surface consistent residual static correction model. This model is based on the following assumption:

- 1) The effect of the static introduces a pure time shift or delay. This delay is a linear phase shift and does not affect amplitude spectrum.
- 2) Surface consistent: each surface location is associated with a constant time delay regardless of the wave path. This is not valid when the near surface layers producing the time shifts are of higher velocity than the layer below.

Based on the above assumptions, a model for travel time t_{ijh} that corresponds to the j th source station, the i th receiver station, and the k th [$k = (i + j)/2$] midpoint

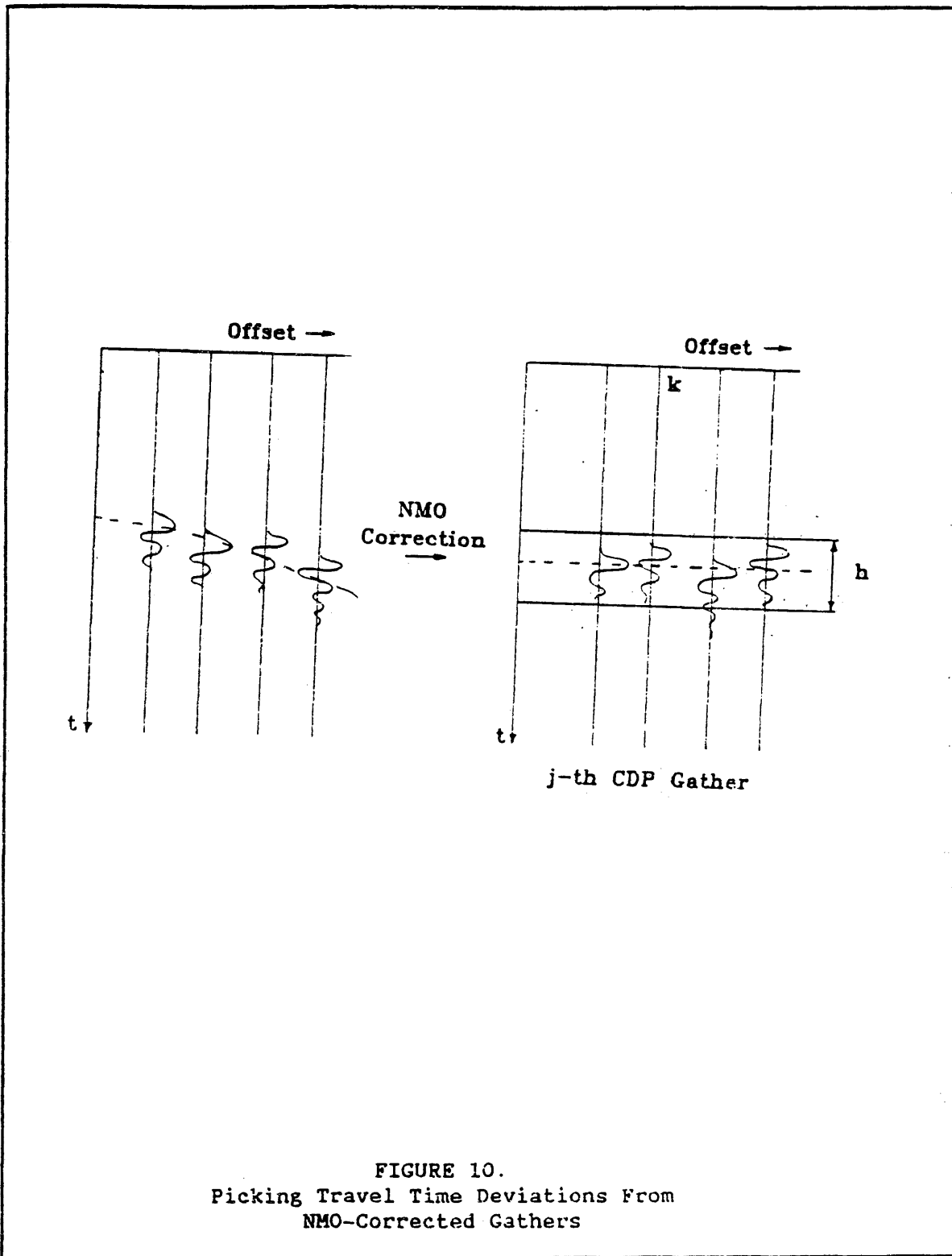


FIGURE 10.
Picking Travel Time Deviations From
NMO-Corrected Gathers

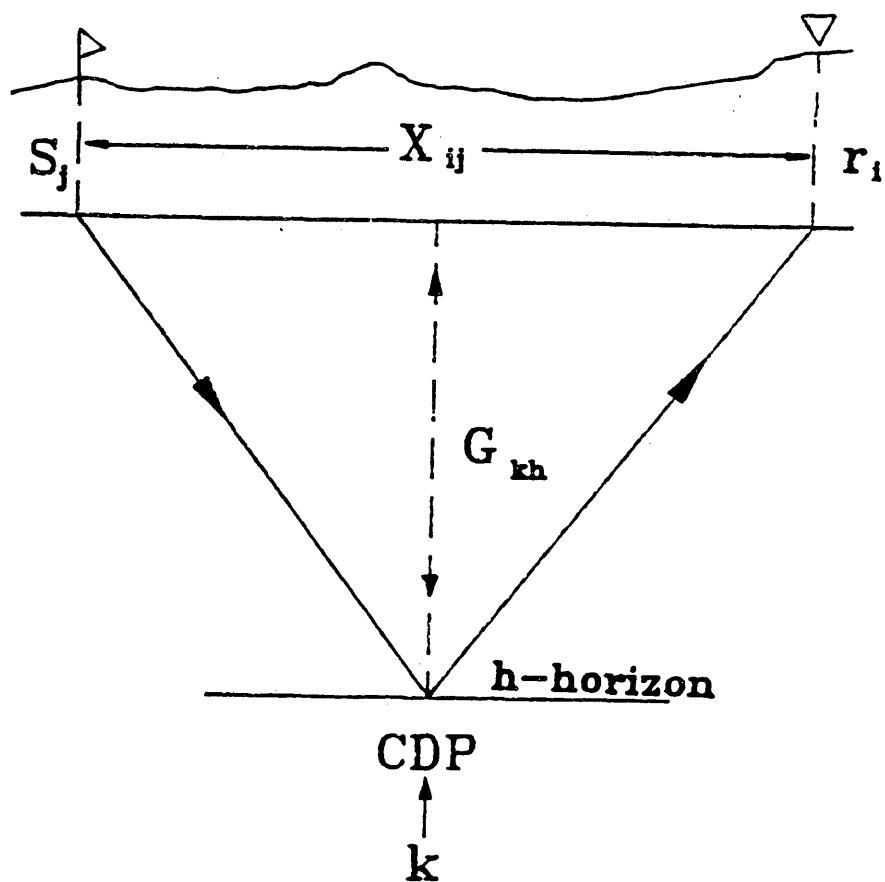


FIGURE 11.
Surface Consistent Statics Model

along the hth horizon can be approximately modeled as

$$t_{ijh} = S_j + R_i + G_{kh} + M_{kh} x_{ij}^2 \quad (1)$$

(see Figure 11)

where:

- S_j = The residual static time shift associated with jth source station.
- R_i = The residual static time shift associated with ith receiver station.
- G_{kh} = The difference in two-way time between the kth midpoint and the reference CMP location along the hth horizon.
- $M_{kh} x_{ij}^2$ = The residual moveout that accounts for the imperfect moveout correction of the hth horizon.

3.2 Scheme of Decomposition

The objective is to decompose the observed travel times from the data (t'_{ijh}) to their individual components as defined by Equation (1). The number of equations is larger than the number of unknowns (individual components). It is not possible to solve for these components exactly. A least square scheme is needed to obtain these unknowns optimally by minimizing the least-square error energy (sum of the squares of residuals).

$$E = \sum_{ijh} (t_{ijh} - t'_{ijh})^2 \quad (2)$$

where

E = error energy

t_{ijh} = observed travel time

t'_{ijh} = estimated travel time

observed time values t_{ijh} is obtained from the data by using a pilot trace scheme (see Yilmaz (1987) p. 196). This scheme estimates the arrival time of reflection at different CMP relative to its location in a reference CMP gather which has a good S/N ratio. This scheme is done by a cross-correlation technique. This time location shift represents the actual time location (G) in addition to effect of error, source static and receiver static and the error in NMO correction.

In order to estimate the components of the time shift, substitute for t_{ijh} from Equation (1) into Equation (2) and minimize the error energy E by using the identities:

$$\frac{\partial E}{\partial S_j} = \frac{\partial E}{\partial r_i} = \frac{\partial E}{\partial G_{kh}} = \frac{\partial E}{\partial M_{kh}} = 0 \quad (3)$$

These equations were solved by Gauss-Seidal methods to estimate source and receiver residual statics locations in addition to the structural term (G_{kh}) and the residual normal moveout correction.

3.3 Residual Static Application.

After computing the individual static shifts associated with each source and receiver location, these shifts are applied to the pre-NMO corrected gather traces. Then the normal processing technique is followed as indicated in Figure 12. The result is MISER Stack Plate 2.

3.4 Results and Further Work

The results of the MISER are: the stack section appears more coherent, resulting in improved quality of section. On the other hand, the MISER cannot accurately resolve static corrections of dimensions greater than one spread length (Wiggins et al. 1976). This can be demonstrated by the existence of the time sag between the station range 9,900-10,400. Therefore, another technique to solve the long wavelength static must be applied. This technique is called "Extended Generalized Reciprocal Method" (EGRM).

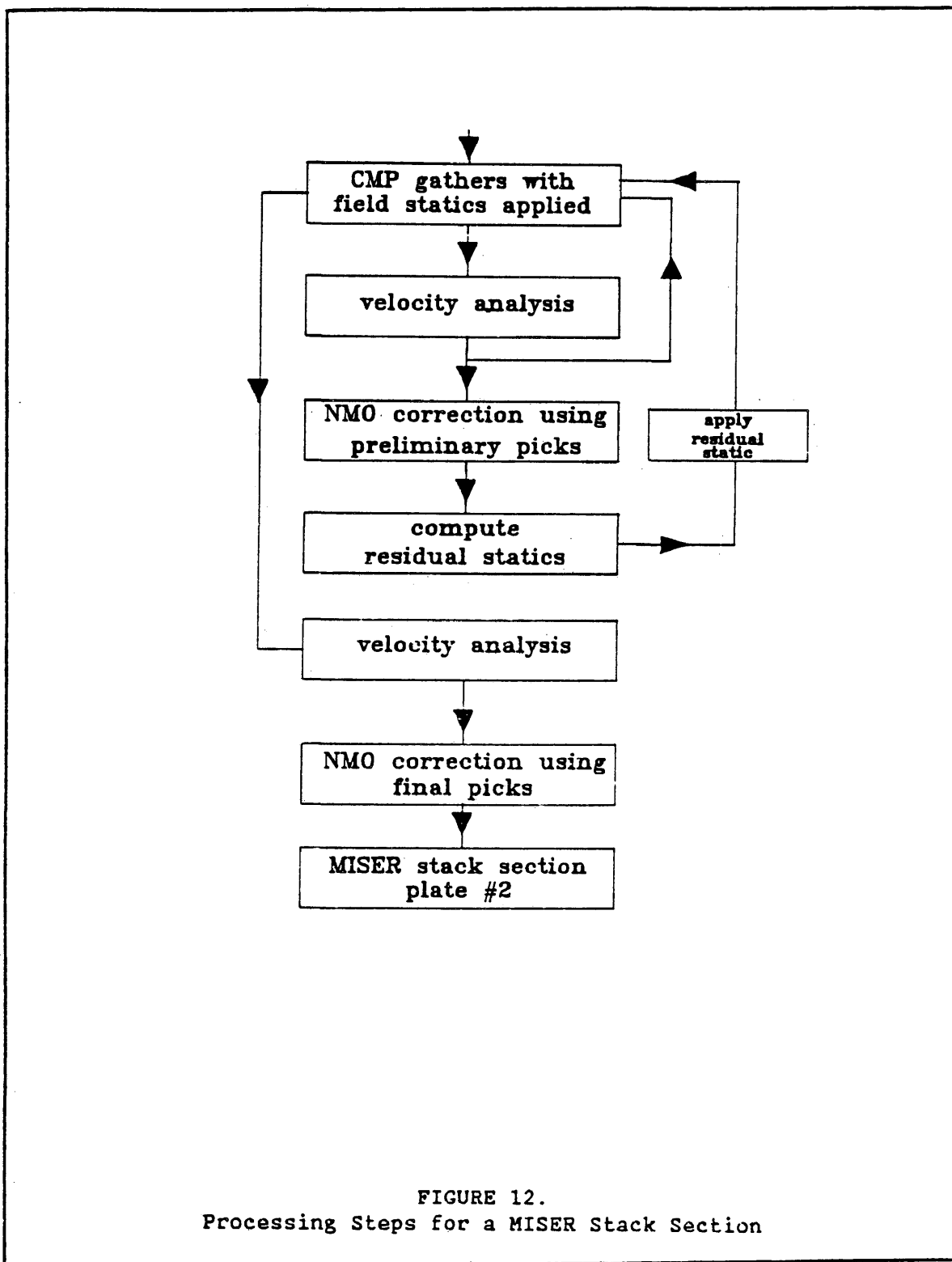


FIGURE 12.
Processing Steps for a MISER Stack Section

4. THE EXTENDED GENERALIZED RECIPROCAL METHOD (ERGM)

4.1 Introduction to the Refraction Theory

The previous discussion and application show that the the automatic reflection static correction (MISER) cannot accurately resolve static corrections at wavelengths greater than one spread length (Wiggins et al. 1976). For this reason, the Extended Generalized Reciprocal Method (EGRM-Western Geophysical) is also used to solve long wavelength static anomalies. The method estimates the near surface velocities by assuming that the static problem on the seismic reflection record is caused by near surface conditions above the deepest refracting interface which is assumed to be the bottom of the weathered layer.

The basic refraction theory describes the refracted arrival time T_{AB} for the single weathering layer case in Figure 13 as:

$$T_{AB} = T_{AC} + T_{CD} + T_{DB} \quad (4)$$

$$T_{AB} = \frac{\overline{AC}}{V_1} + \frac{\overline{CD}}{V_2} + \frac{\overline{DB}}{V_1}$$

\overline{AC} = Distance along ray path between the surface at Point A and the refractor at Point C.

\overline{BD} = Distance along ray path between the surface at Point B and the refractor at Point D.

\overline{CD} = Distance along raypath on refractor between Point C and Point D.

V_1 = Compressional velocity of the medium between the surface and the refractor (weathering velocity).

V_2 = Compressional velocity of the medium immediately underlying the refractor.

Equation (4) could be arranged to be

$$T_{AB} = \frac{ZA \cos\alpha}{V_1} + \frac{\overline{AB}}{V_2} + \frac{ZB \cos\alpha}{V_1} \quad (5)$$

ZA = Thickness of layer 1 beneath Point A.

ZB = Thickness of Layer 1 beneath Point B.

AB = Distance on the surface between A and B

α = Critical angle defined by Snells Law = $\text{Arcsine} \left(\frac{V_1}{V_2} \right)$

Equation (5) is a convenient expression for time AB.

Refraction time can be thought of as consisting of a combination of the time thickness $\frac{Z_1}{V_1}$ at Point A and Point B plus the offset (AB) divided by the refractor velocity, in this case, V_2 (see Figure 13).

4.2 Application of EGRM Method

To apply the EGRM Method the following steps were taken:

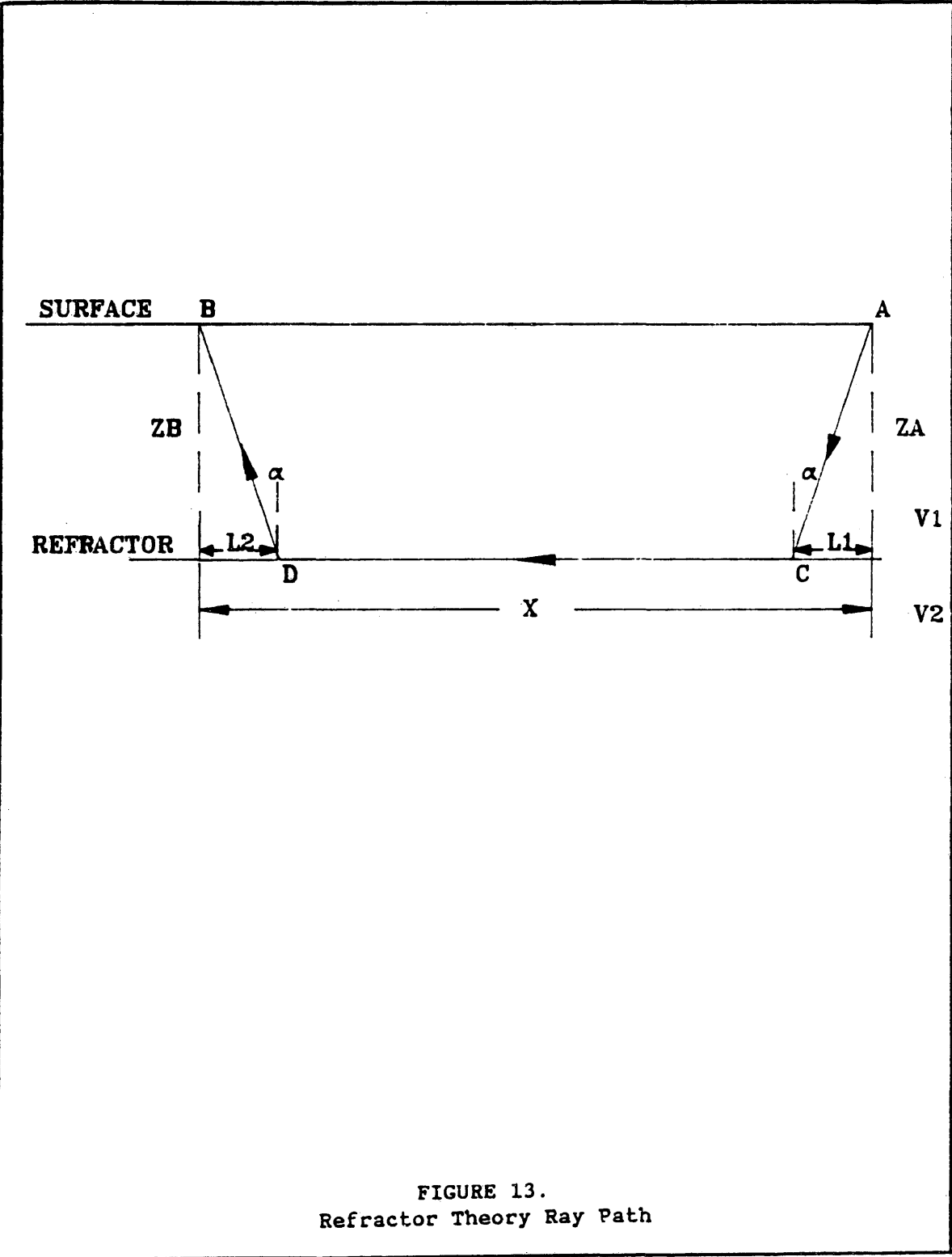


FIGURE 13.
Refractor Theory Ray Path

1. Examine first breaks, they should exist for a large number of shots in the line.
2. Pick the first breaks.
3. Refractor velocity is calculated from time picks under each station on the line.
4. Time depth to the refractor is calculated at each station on the line by using EGRM method.
5. Refractor elevation at each station is obtained from uphole lithology study then the weathering velocity is calculated from the time depth and refractor velocity results.
6. Static correction is calculated.
7. EGRM stack section is obtained.

4.2.1 First Break Existence

It is essential to have good first breaks in order to apply the EGRM theory. In this project, a display record corresponding to each shot was prepared. Record samples of seven shots, one cable-length apart, are shown in Figures 8 and 9 to demonstrate the existence of good first breaks.

4.2.2 Picking the First-Breaks

An automatic picker program is used to pick the first-breaks after a linear Move Out (L.M.O.) correction to the shot gather is carried out. The purpose of L.M.O. correction is to compensate for the effect of offsets, but does not eliminate residual statics. The L.M.O. correction to the entire line will be carried out for every shot in the line by choosing a constant time window above and below the first-break and a constant velocity of 16500 ft/sec. This velocity was arrived at from the average slope of the first breaks of all the shots. As an example, Figure 14 shows one shot record before L.M.O. correction which has a window of 300 ms above and 300 ms below the first-break. The same record is shown in Figure 15 after NMO correction is applied.

The next step after L.M.O. correction application to every shot record is to view the L.M.O. corrected first breaks for the entire line by choosing a trace from each shot record and combining all the traces in a new record. All the traces in the new record have the same offset. This process is performed by a routine called "Seismic Data Coordinate Transform Display" (SDCT). Plate 3 shows eight displays of this routine at eight different offset

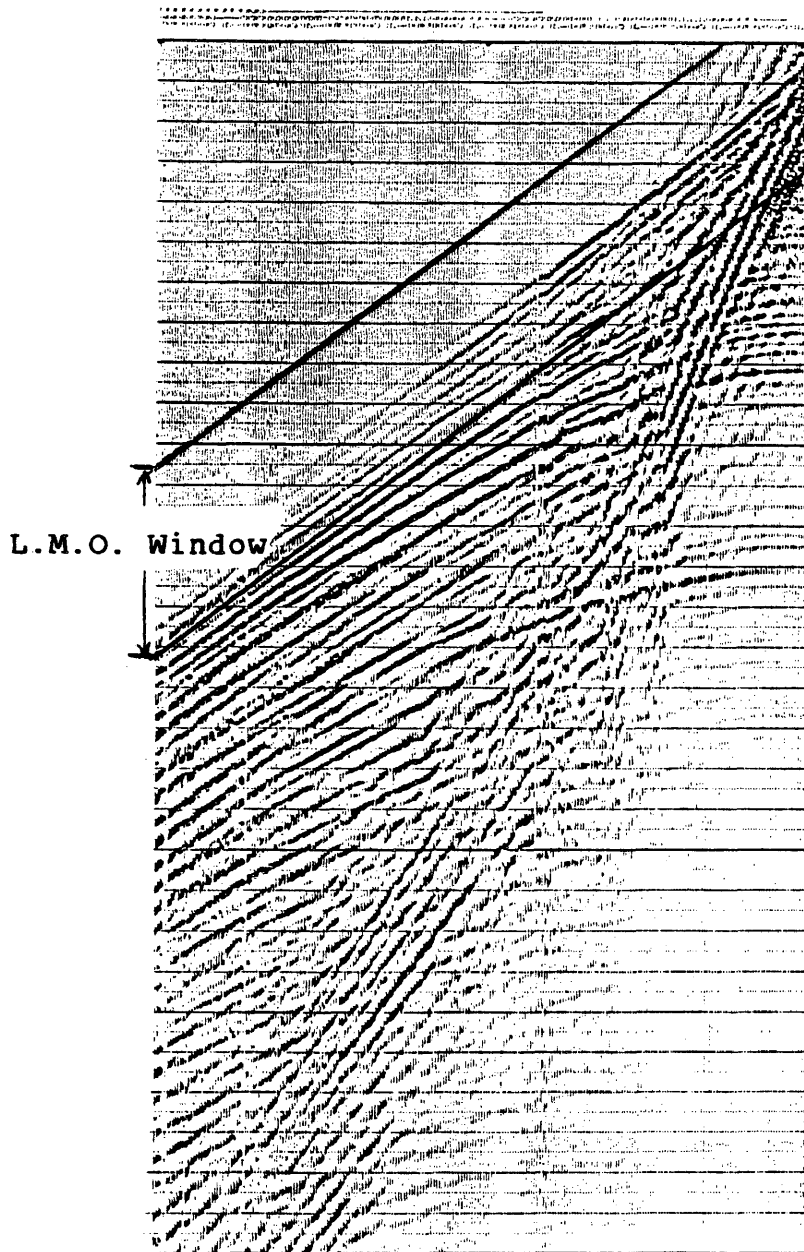


FIGURE 14.
A Shot Record With L.M.O. Window

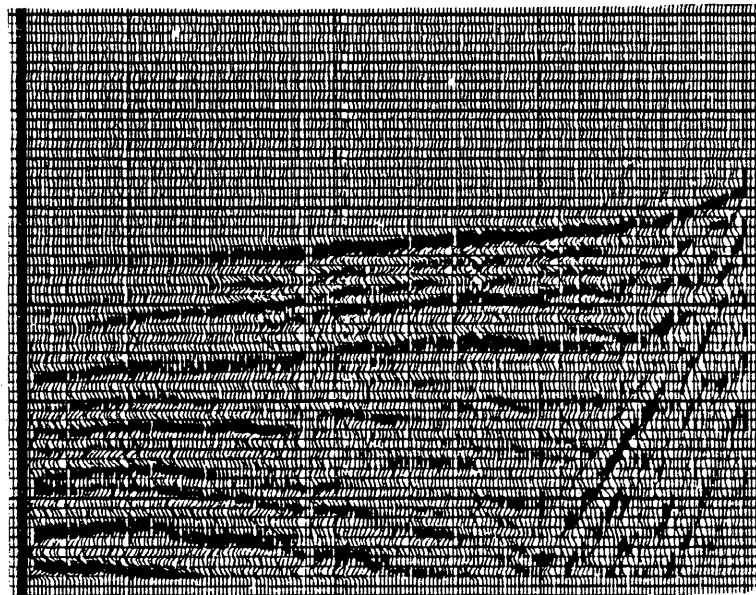


FIGURE 15.
The Same Shot After L.M.O. Correction

distances as shown in that plate. A limited time window of only 600 ms is shown in each offset display in Plate 3. The first display, for example, has an offset of 3,252 ft and consists of two axis. The display axis contains a sequence of L.M.O. traces stacked side-by-side. The first trace in that display is L.M.O. corrected and picked from the first shot in the line at an offset of 3,252 ft and placed in its actual surface coordinate location. The adjacent trace to it came from the next adjacent sequence shot and so on to cover the entire line.

The purposes of the SDCT display are:

1. The results of digitization of SDCT displays will be used as a guide to the automatic picker program at each shot. For example, if three SDCT displays are digitized for the same line with different offsets, the automatic picker program can provide three reference points for each shot to enhance its ability of picking first break events.
2. From the SDCT offset display the offset range for the time depth calculation can be determined. This range is greater than the critical distance.

3. Lateral extents of static anomalies can be determined from the SDCT display. Also, the surface consistency assumptions for both shots and receivers can be analyzed. Some of the static anomalies appearing in all offset windows corresponding to the same shot location can be assumed to originate from a velocity anomaly under that shot.

As a result of the automatic picker program, a display of Plate 4A shows the desired refracted arrival times at a constant offset range for each shot for the entire line displayed side-by-side. The shape of straight parallel refractor lines for all the shots indicate that there is only one flat refractor.

4.2.3 Refractor Velocity Calculation

To calculate the refractor velocity V_{n+1} for off-end shooting line similar to this problem, reciprocity is assumed. As shown in Figure 16, A is the starting point, B is the ending point. The velocity analysis routines compute the travel time difference to each of the five stations G1, G2, G3, G4 and G5 and analyze these differences relative to associated differences in offset

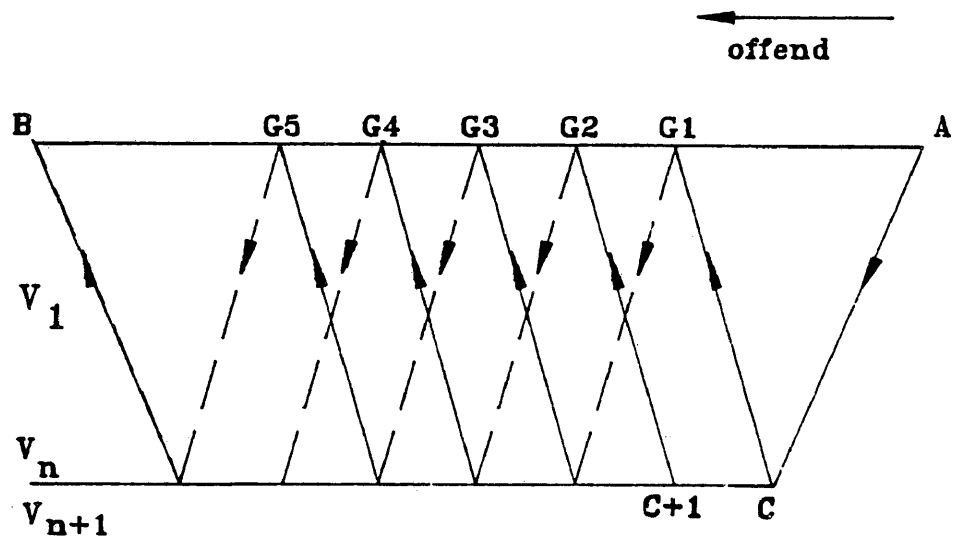


FIGURE 16.
Refractor Velocity Ray Path

distances. In other words, for Station G5, the difference in arrival times from A to G5, and B to G5, would be a positive value

$$\text{Diff (Time)} = T_{AG5} - T_{BG5} > 0$$

Likewise, the difference in offset distances from A to G5 and B to G5 would be a positive value so

$$\text{Diff (offset)} = \overline{AG5} - \overline{BG5} > 0.$$

Similarly, the difference in arrival times from A to Station G₁ would be a negative value as would the difference in offset distances.

$$\text{Diff (time)} = T_{AG1} - T_{BG1} < 0$$

$$\text{Diff (offset)} = \overline{AG1} - \overline{BG1} < 0$$

since Station G3 is about equal distance from source locations A and B, both the arrival time difference and offset distance differences will be approximately zero.

This analysis is shown graphically in Figure 17 where differences in arrival times were plotted versus differences in offsets for the above example. One-half of the inverse of the slope of the least square fit through the five points in Figure 17 would be an estimate of the velocity of refractor between Stations A and B. This estimated velocity will be assigned to the point on the

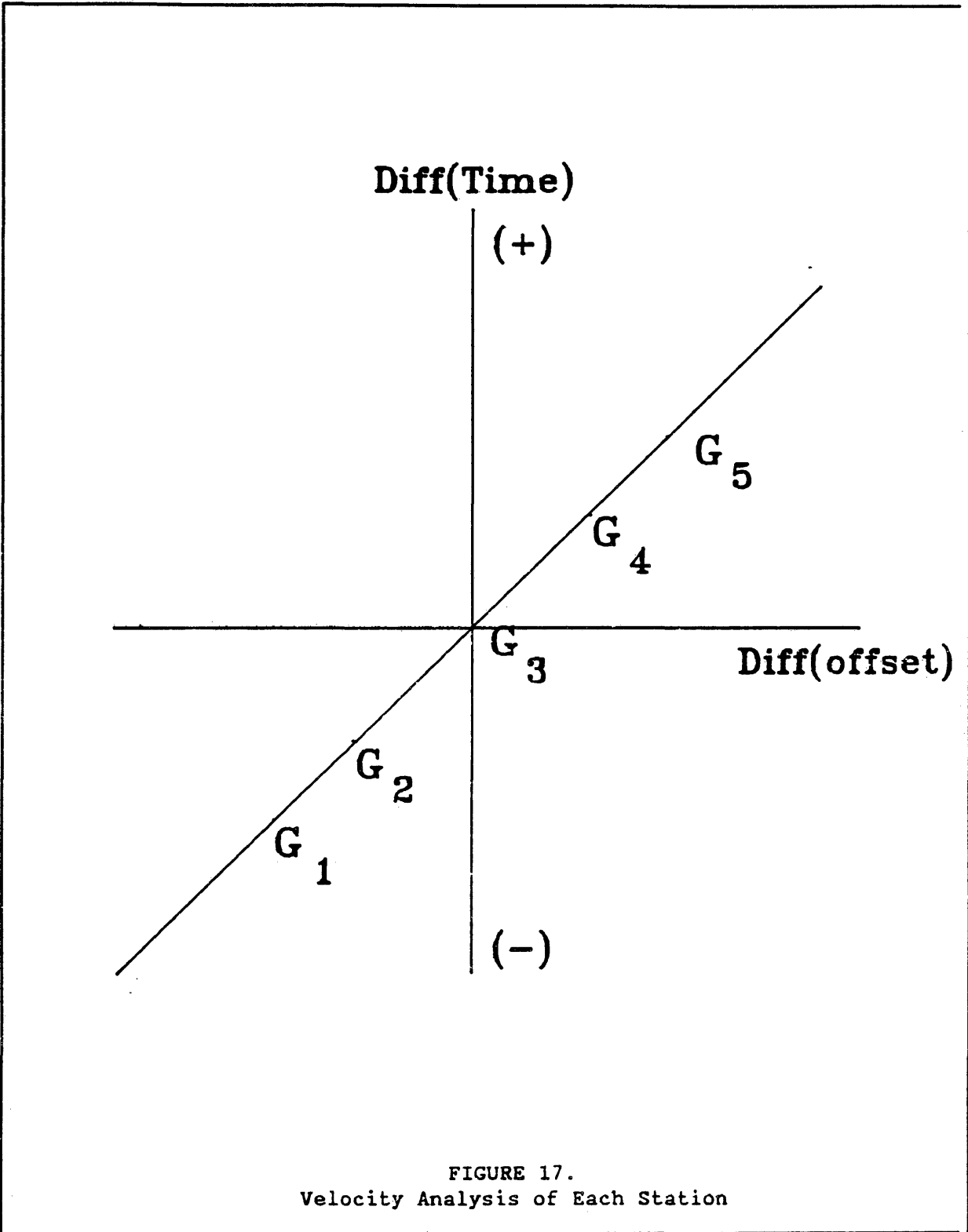


FIGURE 17.
Velocity Analysis of Each Station

refractor directly under Surface Station C. As sources A and B move to locations A+1 and B+1, the new calculated velocity will hold for location C+1 on the refractor and so on to cover the entire line. As a result of this analysis, Plate 5A shows the refractor velocity profile distribution for the entire line. This is also shown in Figure 18.

4.2.4 Time Depth Computation

The EGRM requires three travel times from two shots to estimate the time-depth at a particular Station G. Assume the shot station configuration as shown in Figure 19. Three travel paths are used to compute the time-depth at Station G on the surface. Travel paths are as follows:

(---) TAG = Travel time from shot at A to the receiver at G or vice versa.

(--.) TGB = Travel time from shot at G to receiver at B or vice versa.

(—) TAB = Travel time from shot at A to receiver at B or vice versa.

The EGRM equation for computing the time-depth at Station G is:

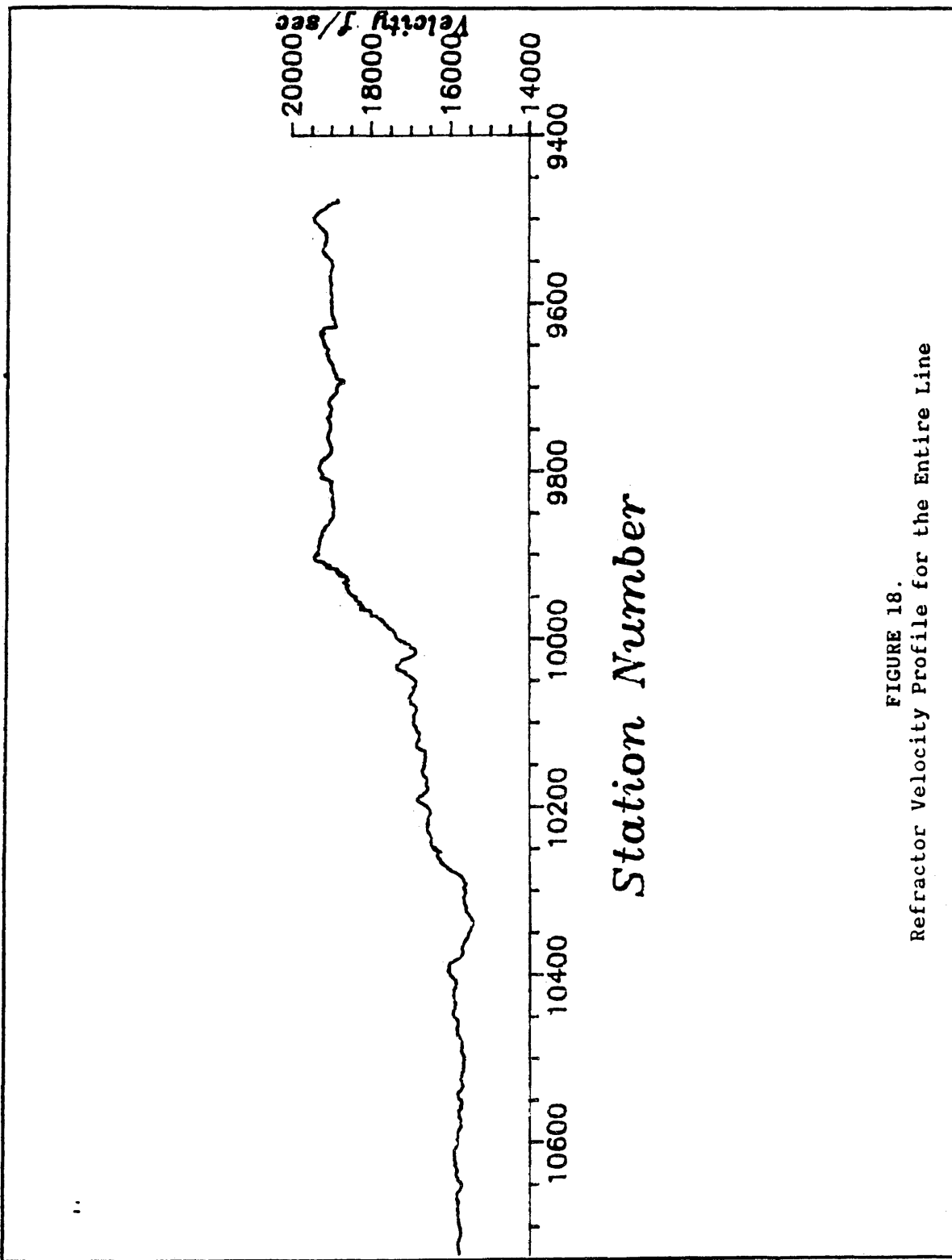


FIGURE 18.
Refractor Velocity Profile for the Entire Line

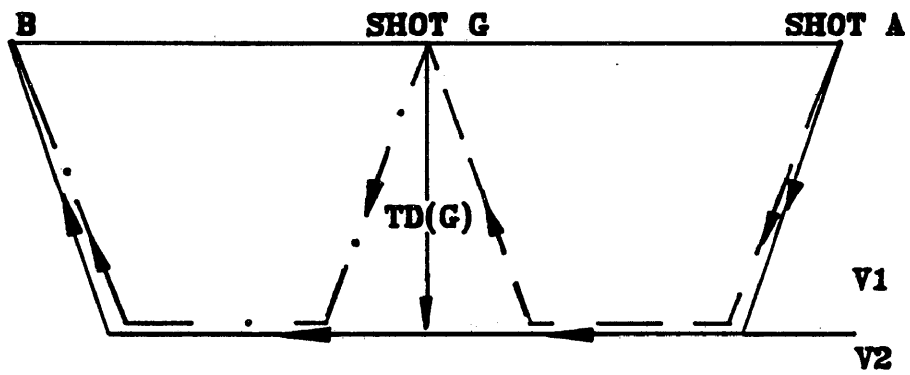


FIGURE 19.
EGRM Time-Depth Ray Path

ARTHUR LAKES LIBRARY
COLORADO SCHOOL of MINES
GOLDEN, COLORADO 80401

$$TD(G) = (TAG + TGB - TAB)/2 \quad (6)$$

Combining Equation 5 and 6 the result is:

$$TD = [ZA * \cos \alpha / V_1 + \bar{AG} / V_2 + ZG * \cos \alpha / V_1 + ZG * \cos \alpha / V_1 + \bar{GB} / V_2 + ZB * \cos \alpha / V_1 - (ZA * \cos \alpha / V_1 + \bar{AB} / V_2 + ZB * \cos \alpha / V_1)] / 2$$

where ZA, ZG, ZB are vertical depth from surface to the refractor at Stations A, G, B, consecutively, a reorganization of the previous equation yields the following equation

$$TD(G) = [2 * ZG * \cos \alpha / V_1 + (\bar{AG} + \bar{GB} - \bar{AB}) / V_2] / 2 \quad (7)$$

However $\bar{AB} = \bar{AG} + \bar{GB}$. Substitution in Equation 7 results in the elimination of the second term which is called the "residual offset term."

The equation reduces to:

$$TD(G) = ZG * \cos \alpha / V_1$$

where TD(G) signifies the one-way vertical travel to the refractor at Station G.

After applying this method to the data, results are shown in Plate 4A. The EGRM time depth can only estimate time depth based on station position and cannot differentiate between shot and detector time depth. Also, there is not sufficient information to estimate time depths at

ends of the line. So the EGRM time-depths can be used as an initial structural solution to solve for time-depth at both ends of the lines, using an iteration method as follows:

$$T_{AB} = T_A + \frac{\text{offset}}{V_{n+1}} + T_B \quad (\text{see Figure 13}) \quad (10)$$

T_A = Time-depth at Source A

T_B = Time-depth at Detector B

$$T_A = T_{AB} - \frac{\text{offset}}{V_{n+1}} - T_B \quad (11)$$

T_B = Picked from seismic record

V_{n+1} = Velocity of the refractor under that offset

T_A = Calculated from EGRM

$$T_B = T_{AB} - \frac{\text{offset}}{V_{n+1}} - T_A \quad (12)$$

First, the shot terms T_A s are re-estimated for every shot on the line using Equation 11 provided that initial estimates for the detector times T_B are known from EGRM. This can be done for every shot on the line after the re-estimation of all the shot terms was produced. Re-estimation of all the detector terms in a similar fashion was performed using Equation 12 (Plate 5D). These shot time depths and detector time depths are used to calculate the EGRM shot static and receiver static.

4.2.5 Refractor Elevation and Weathering Velocity

Uphole survey is a common method in the industry to determine the weathering velocity. For economical as well as logistical reasons only four upholes were drilled in the area. Figure 20 shows the location and depth of these upholes in the elevation profile. Studying the lithology of these upholes resulted in defining a thick limestone layer of approximate thickness of 250 ft and apparent dip of $\approx 0.3^\circ$ to the east. This layer is considered to be a refracting layer. From the surface elevation and refractor interpolated elevation, a weathering thickness is calculated and weathering velocity is obtained using this equation:

$$V_1 = \frac{V_2 * Z_1}{(TD^2 * V_2^2 + Z_1^2)^{1/2}}$$

where: V_2 = Refractor velocity

Z_1 = Thickness of weathering

TD = Time depth at each station

Plate 5A and Figure 21 show the weathering velocity profile for the entire line under each station.

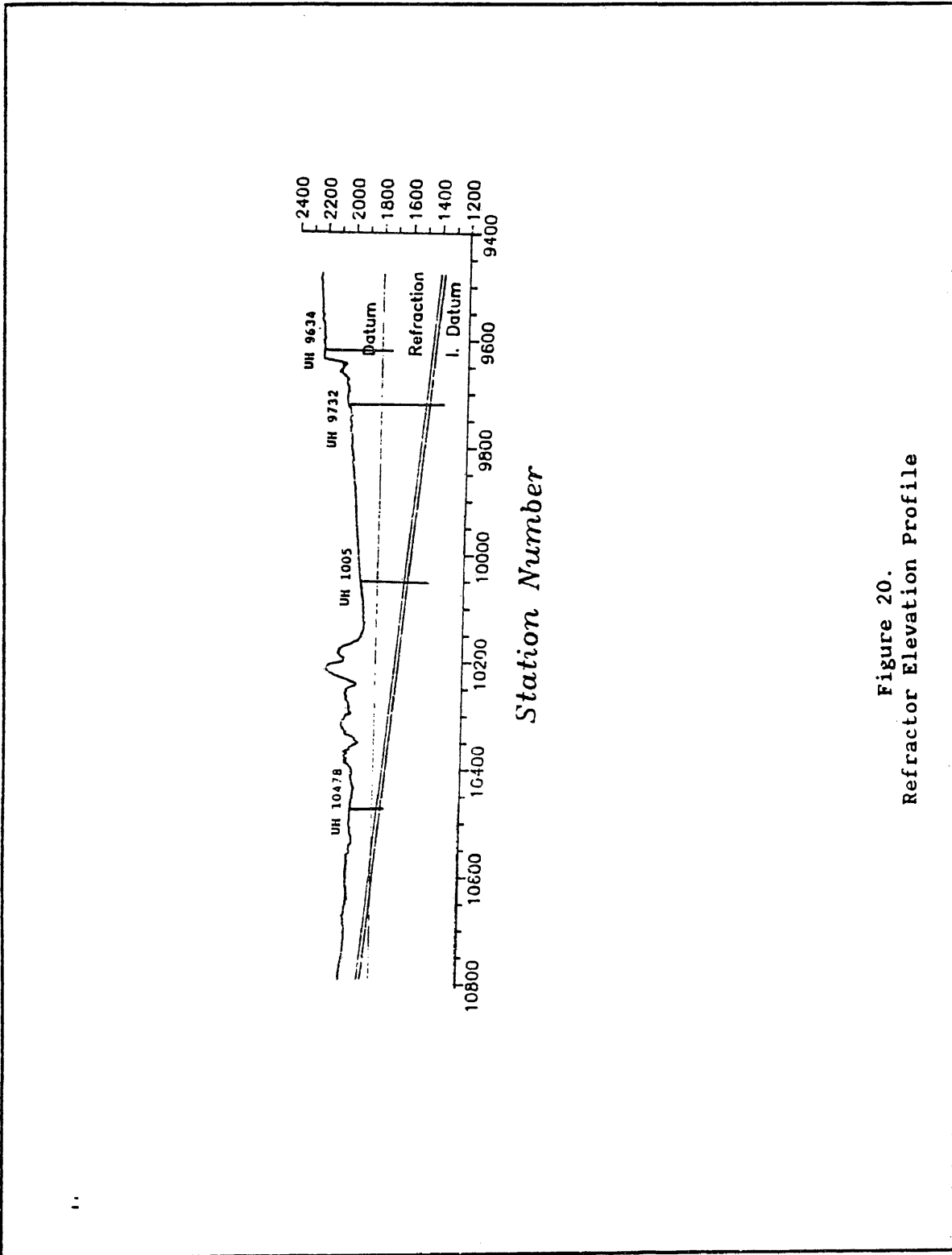


Figure 20.
Refractor Elevation Profile

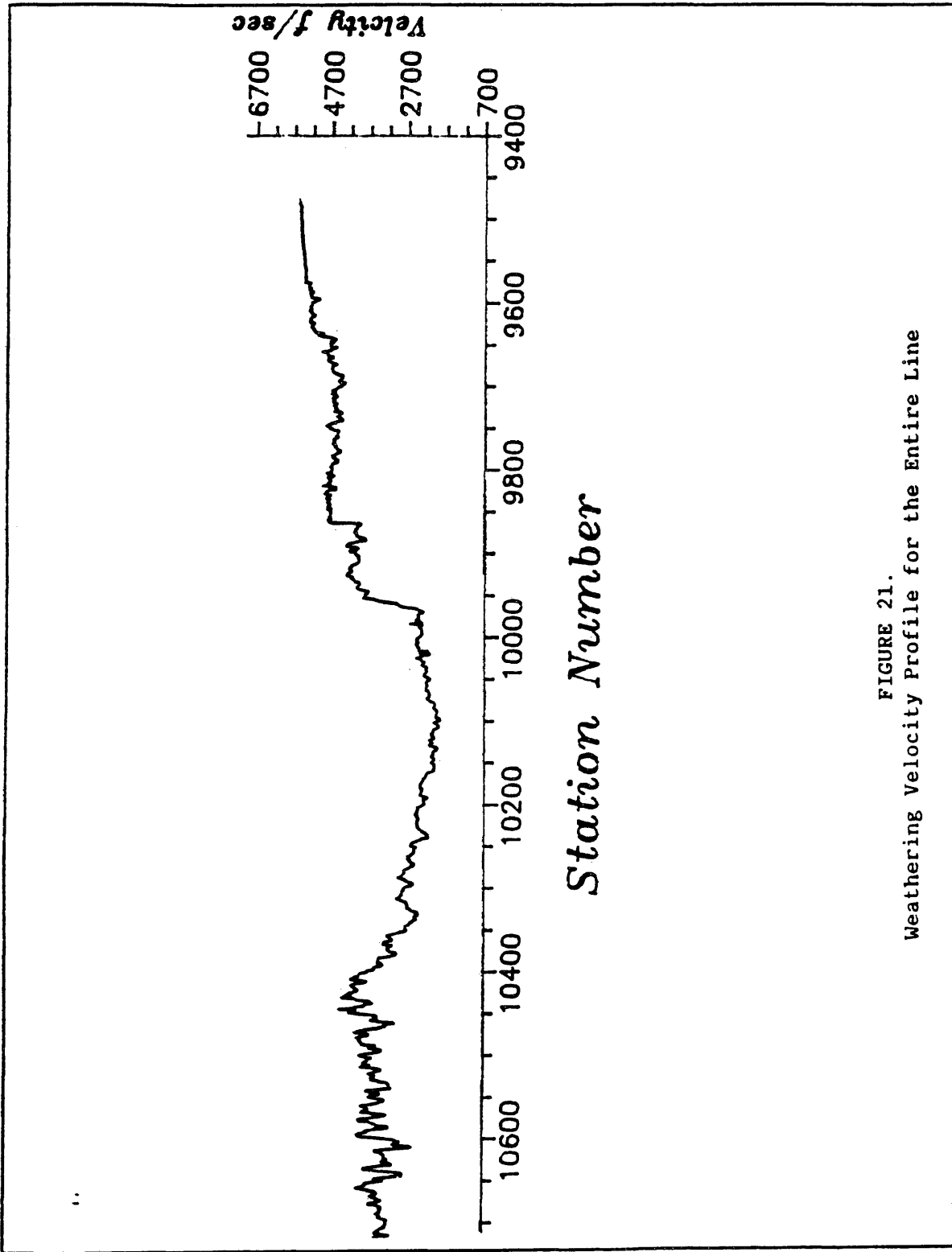


FIGURE 21.
Weathering Velocity Profile for the Entire Line

4.2.6 Static Computations

The static correction, as defined in this report, is the sum of a series of corrections which are equivalent to movements to consecutive surfaces. The first movement is the vertical time delay from the surface to the refractor. The second is the vertical time delay from the refractor to a specified intermediate datum. The final movement is from the intermediate datum to a final datum at a laterally constant replacement velocity. The purpose of final movement is to stack the data at a desired datum elevation. The static computation equation for a refractor layer in Figure 20 at any station on the line is shown below.

$$T_s = \text{Thick}(W)/V_W + (ER-EI)/V_R + (EI-ED)/V_r$$

T_s = Total static at a station

$\text{Thick}(W)$ = Thickness of weathering layer

V_W = Velocity of weathering

ER = Elevation of refractor

EI = Elevation of intermediate datum

V_R = Refractor velocity

ED = Elevation of final datum

V_r = Replacement velocity

Plate 5D is a display of the EGRM static result for this project. The symbol () represents the shot static and symbol (*) represents the receiver static at the same station number for the entire line. Also, Figures 22 and 23 show the shot and receiver static profile for the entire line under each station. Notice that both shot and receiver static graphs resemble each other but differ somewhat at some station locations due to different elevation to shot and receiver in that station location or absence of shot or geophone at that station location.

Plate 5C is a result difference between the (EGRM) static result and the (MISER) static result in Chapter 3, above. For example, if the difference between EGRM and MISER at a certain station is zero, this means both have the same solution at that station. If the difference is large, this means that the EGRM detected a static problem in this area that MISER cannot distinguish.

4.3 EGRM Stack Section

Plate 6 shows the result of application of the refraction static to the data according to processing steps in Figure 24. It is obvious that the time sag is almost eliminated. The long wave length treatment

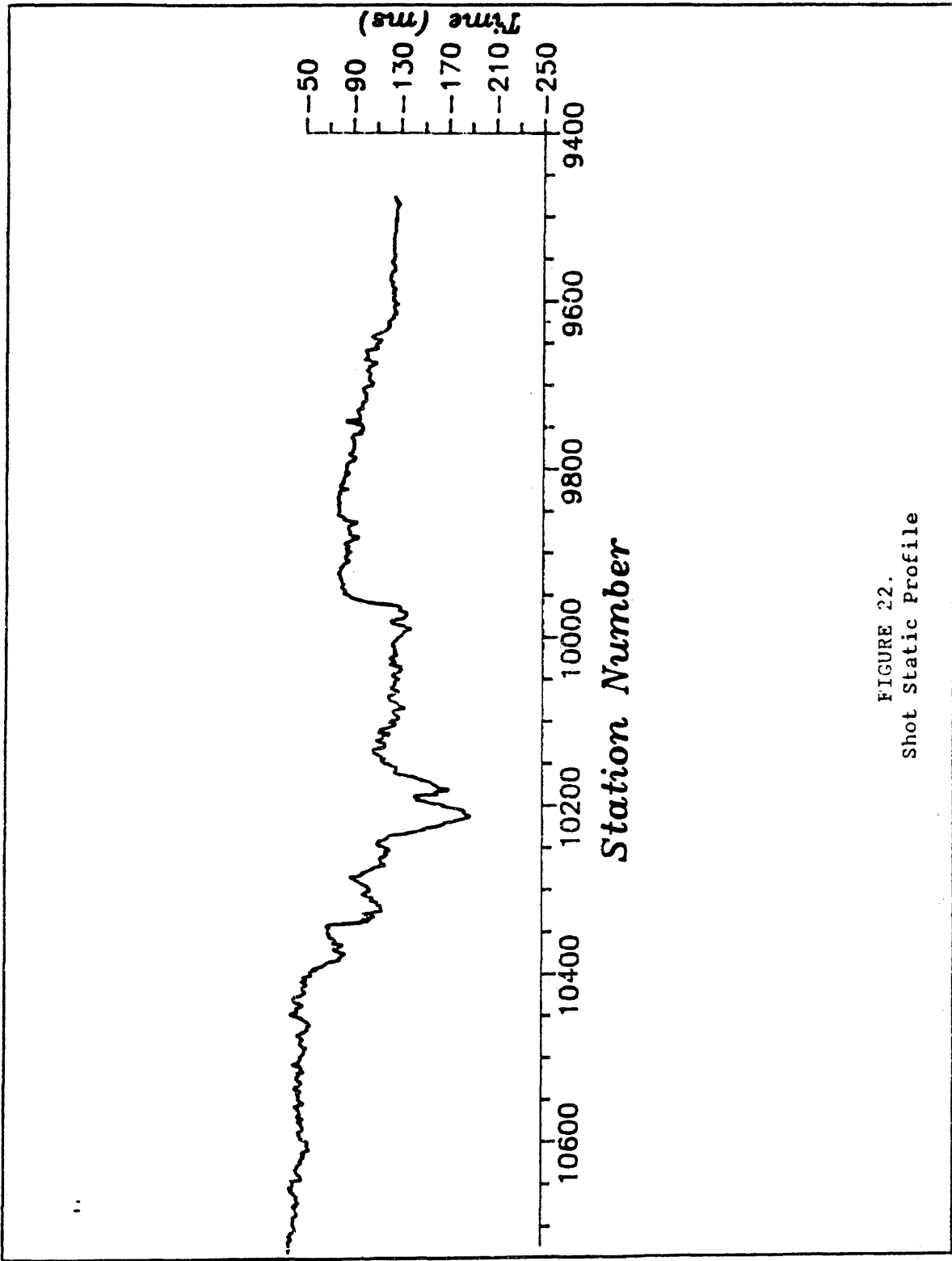


FIGURE 22.
Shot Static Profile

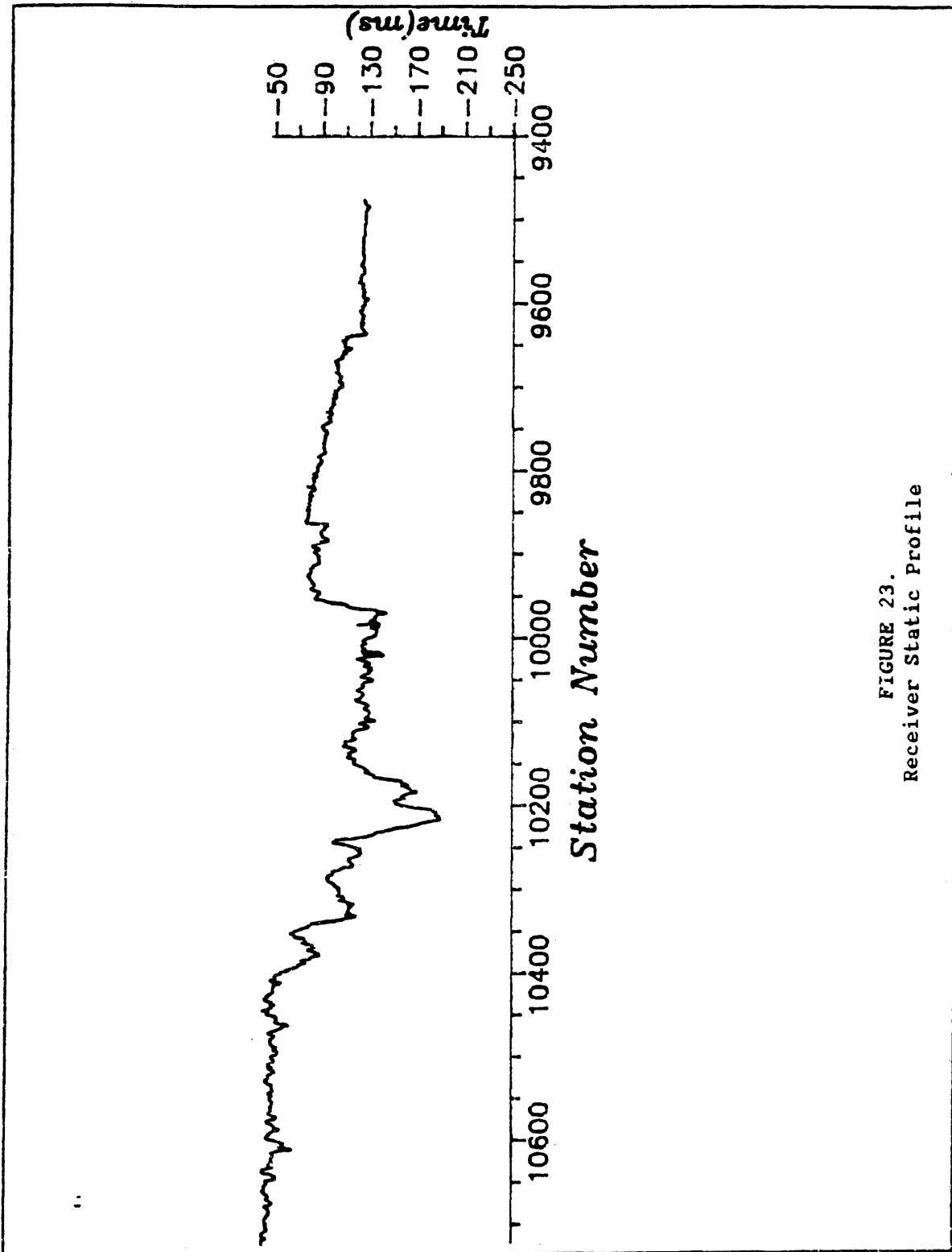


FIGURE 23.
Receiver Static Profile

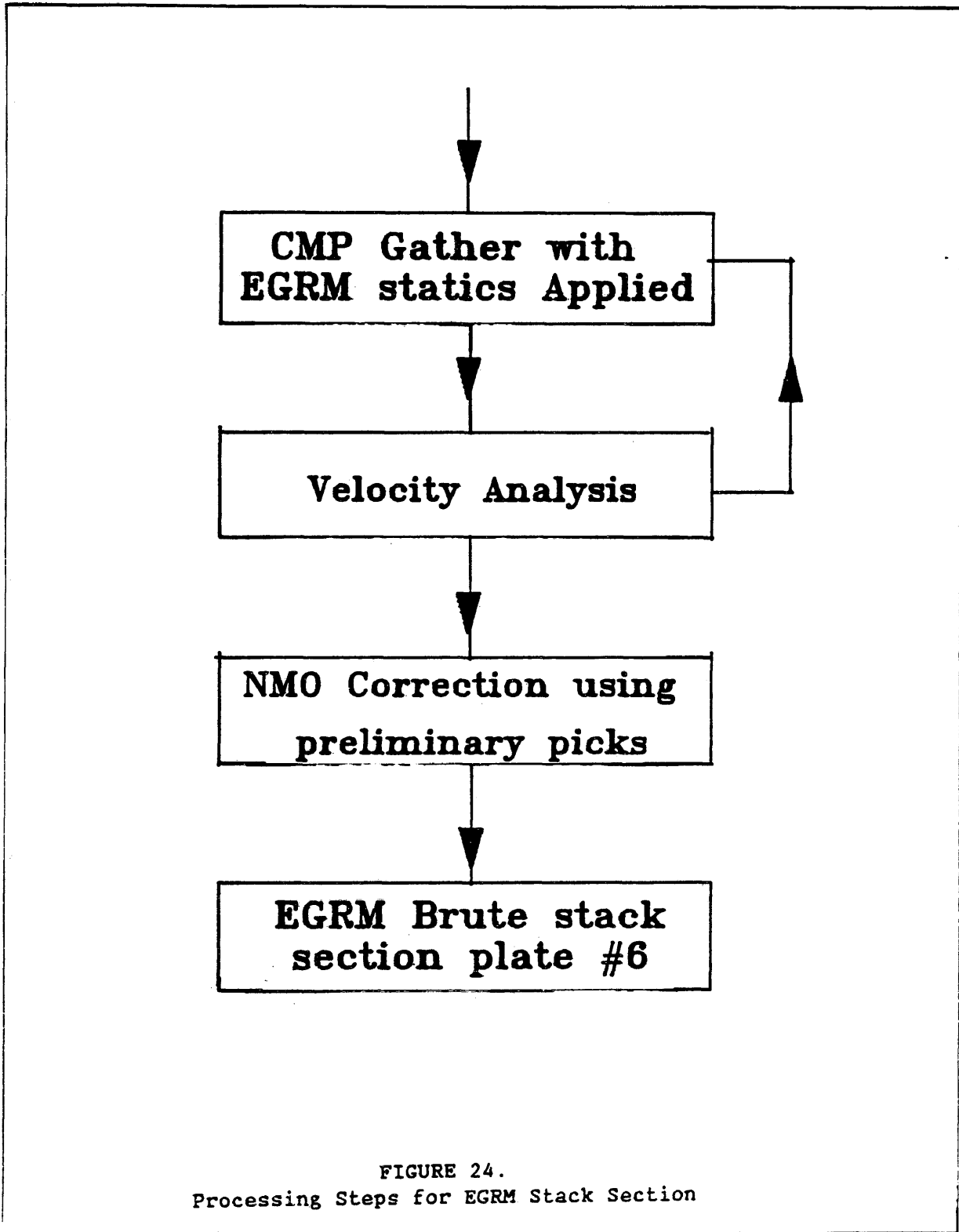


FIGURE 24.
Processing Steps for EGRM Stack Section

improved continuity and wavelet coherency and has removed near surface distortions related to subsurface inhomogeneities.

5. MISER TO EGRM

Plate 7 is a stack section after application of refraction static corrections followed by application of residual reflection static corrections (MISER). Processing steps are shown in Figure 25. In both stages, (EGROM MISER) the timing corrections are surface-consistent. The result of this combined process shows slightly improved reflection continuity over that in the stack shown in Plate 6.

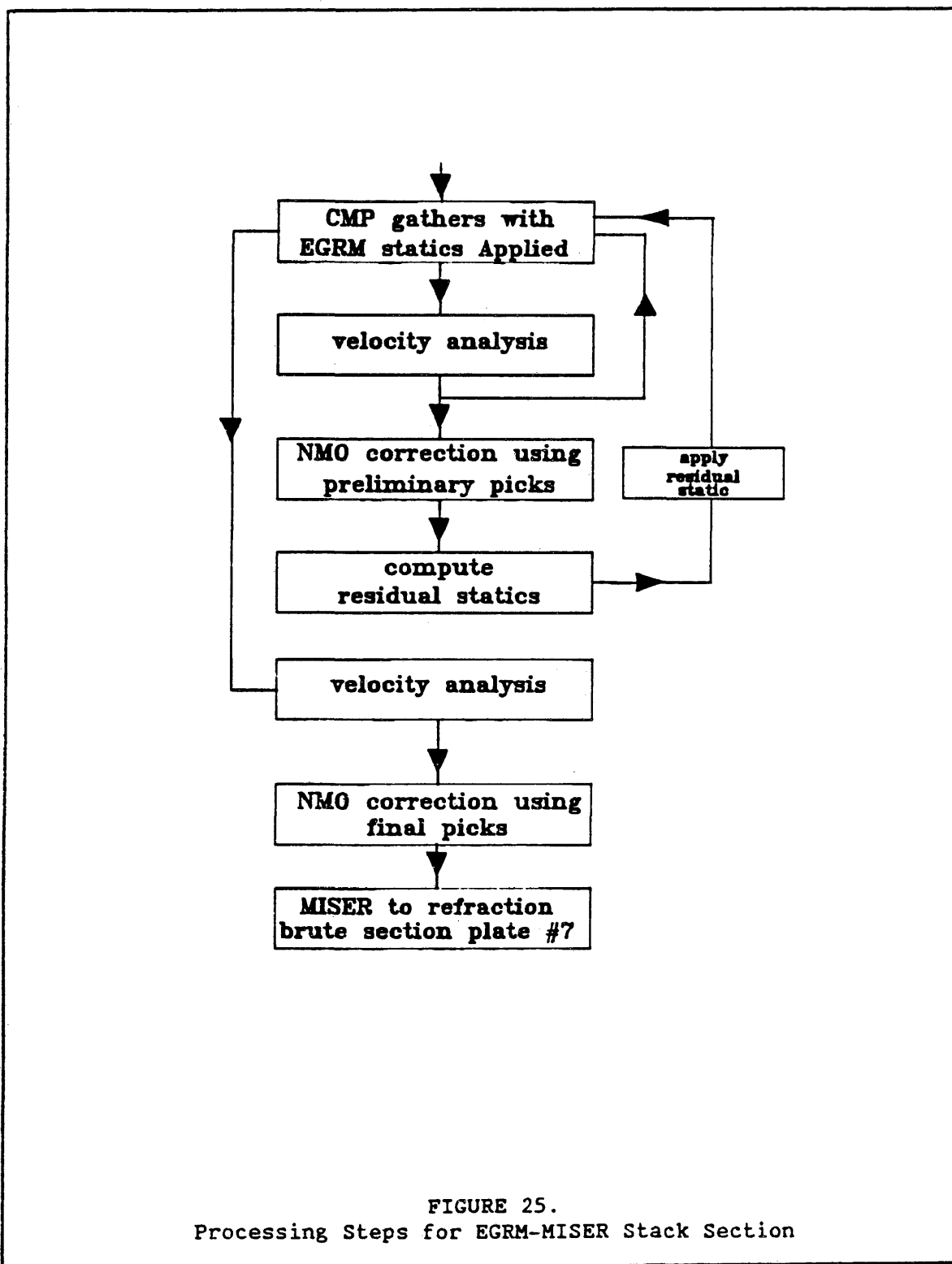


FIGURE 25.
Processing Steps for EGRM-MISER Stack Section

6. CONCLUSION

In conclusion, the EGRM method of Western Geophysical is capable of solving long wave length static problems where the refractor elevation from geologic and upholes information is provided. Weathering velocity and other parameters such as time depth and refractor velocity are extracted from EGRM application. All these parameters are reasonable and match the surface and subsurface geology. The application of the static values from the above parameters give a coherent EGRM brute stack section. MISER software cannot solve long wave length problem because it depends on a time shift between CMP gathers in a short wave length basis. On the other hand, MISER gives good results when it applied after EGRM application to solve the remaining short wave length static as a final step of static correction.

REFERENCES

- Diggins, Chuck, Carvill, Charles, and Daly, Cathal, A Hybrid refraction algorithm, Western Geophysical Division, Western Atlas International, Inc., In press.
- Daly, Cathal, and Diggins, Chuck, The use of refractor elevation models in the computation of refraction statics, Western Geophysical Company, Division of Western Atlas International, Inc., In press.
- Hawkins, L.V., 1961, The reciprocal method of routine shallow seismic refraction investigations: Geophysics, 26, 806-819.
- Heiland, C.A., 1940, Geophysical Exploration: New York, Prentice-Hall.
- Hileman, V.A., Embree, P., and Pfleuger, V., 1968, Automated static corrections: Geophysical Prospecting, 16, 326-358.
- Ozdongun, Yilmaz, 1987, Seismic data processing.
- Palmer, D., 1980, The generalized reciprocal method of refraction seismic interpretation: Tulsa, Society of Exploration Geophysicists.
- Palmer, D., 1981, The generalized reciprocal method of refraction seismic interpretation: Geophysics, 46, 1508-1518.
- Taner, M.T., Koehler, F., and Alhilali, K., 1974, Estimation and Correction of near-surface time anomalies: Geophysics, 39, 441-463.
- Wiggins, R., Larner, K., and Wisecup, R.D., 1976, Residual statics analysis as a general linear inverse problem: Geophysics, 41, 922-938.

PLATE
VIB. PTS. 9477-10775
NO REFRACTION BRUTE

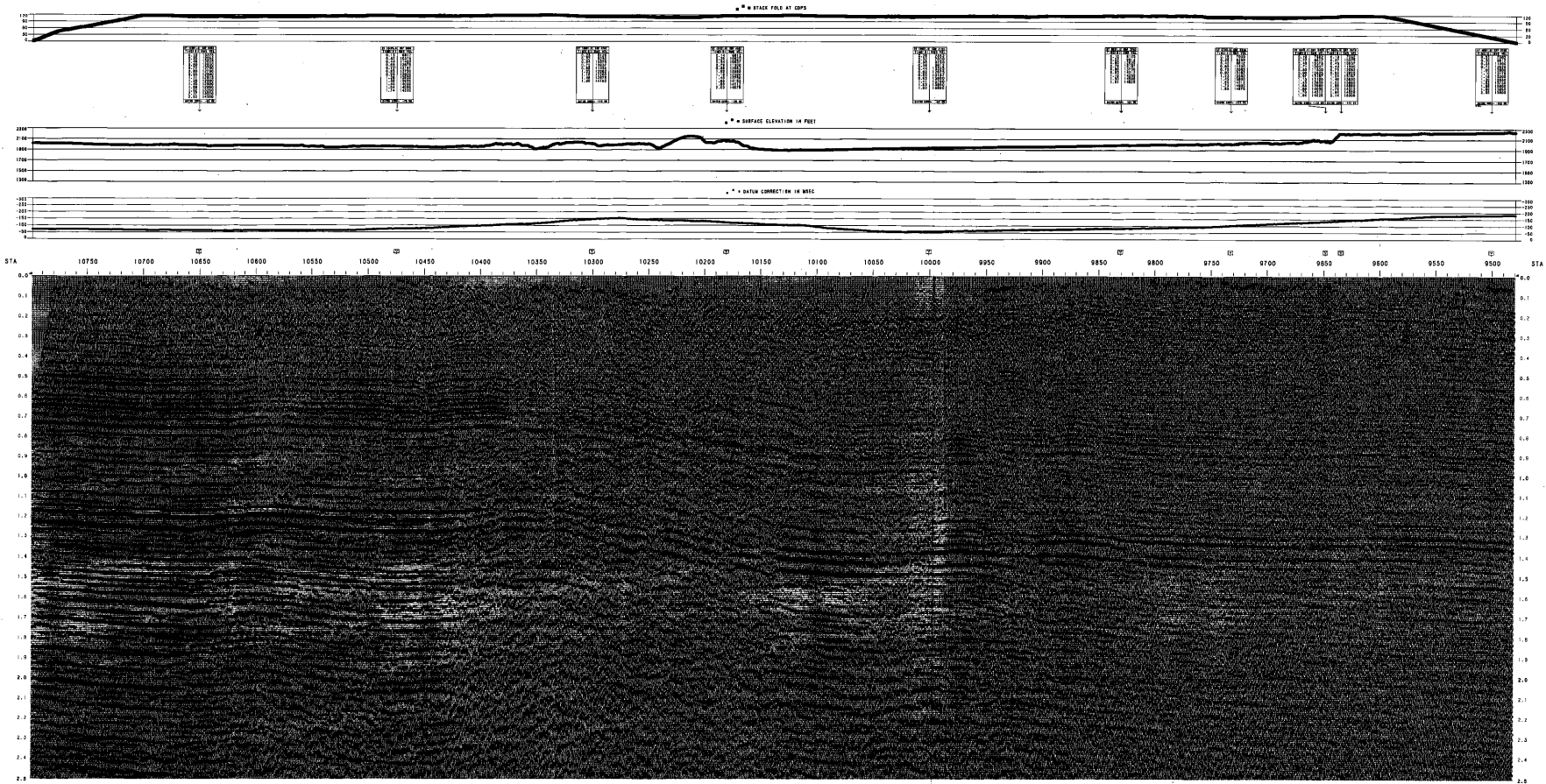


PLATE 1
VIB. PTS. 9477-10775
NO REFRACTION BRUTE
TRISSER AL-YACOUB
ER-3574

WEST

PLATE # 1

TRISSER AL-YACOUB
ER-3574

SEISMIC VELOCITY: 1000 FT/SEC
VIB. PTS.: 9477-10775
SEIS. DIGITAL CENTER: JUN 15 1964

RECORDING INFORMATION:

RECORDING UNIT: 1000 FT/SEC
RECORDING TIME: 10:00 AM
RECORDING DATE: JUN 15 1964

SEISMIC INFORMATION:

SEISMIC VELOCITY: 1000 FT/SEC
VIB. PTS.: 9477-10775
SEIS. DIGITAL CENTER: JUN 15 1964

REVISIONS:

1. ORIGINAL RECORDING
2. REVISIONS
3. REVISIONS
4. REVISIONS
5. REVISIONS
6. REVISIONS
7. REVISIONS

WESTERN GEOPHYSICAL

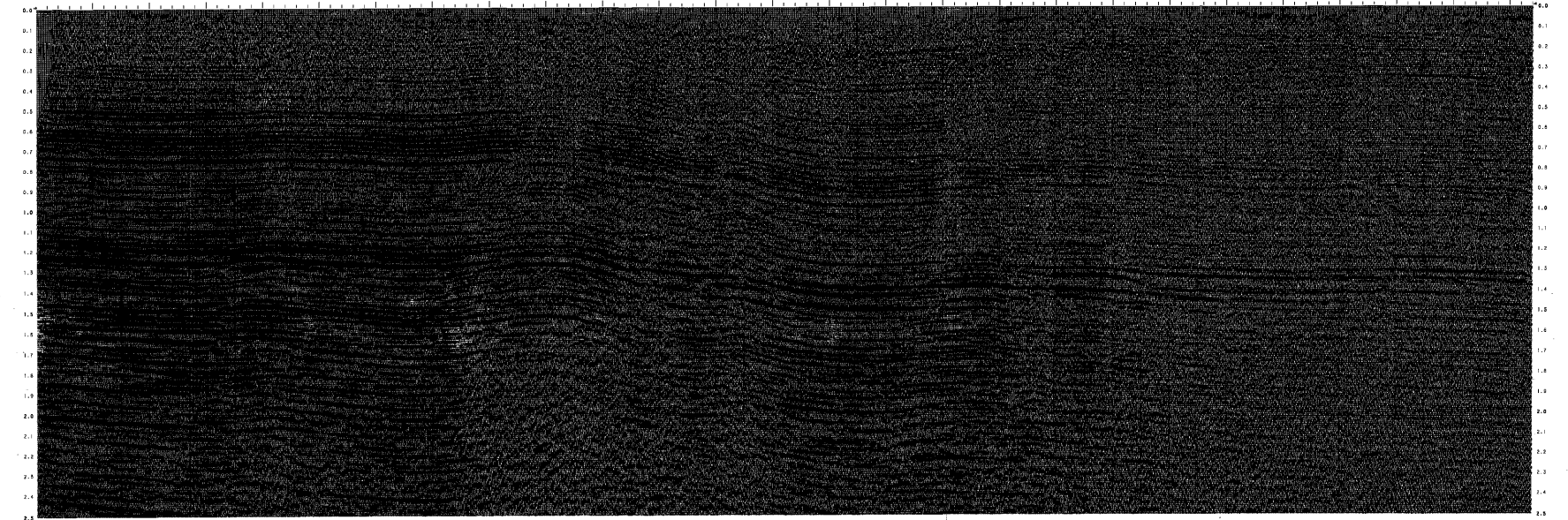
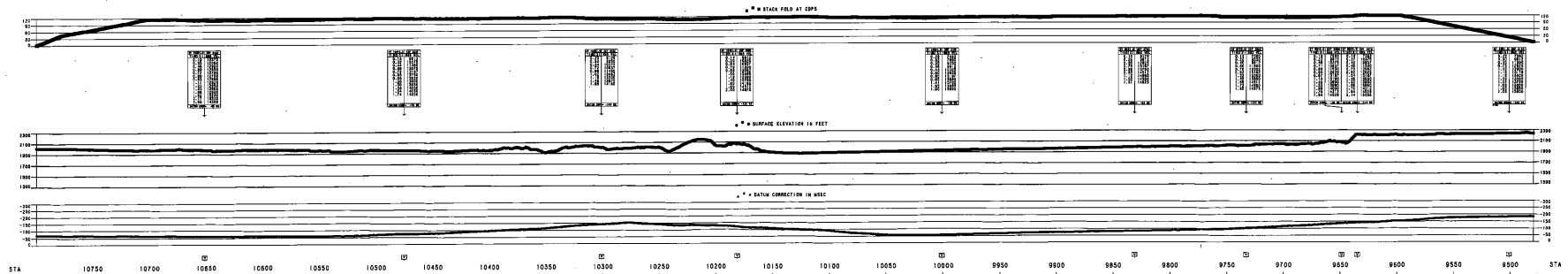
CONSTRUCTION REQUIREMENTS:

1. RECORDING UNIT: 1000 FT/SEC
2. REVISIONS: 1000 FT/SEC
3. REVISIONS: 1000 FT/SEC
4. REVISIONS: 1000 FT/SEC
5. REVISIONS: 1000 FT/SEC
6. REVISIONS: 1000 FT/SEC
7. REVISIONS: 1000 FT/SEC

REVISIONS:

1. REVISIONS: 1000 FT/SEC
2. REVISIONS: 1000 FT/SEC
3. REVISIONS: 1000 FT/SEC
4. REVISIONS: 1000 FT/SEC
5. REVISIONS: 1000 FT/SEC
6. REVISIONS: 1000 FT/SEC
7. REVISIONS: 1000 FT/SEC

HORIZONTAL SCALE: 1 IN = 1000 FT
VERTICAL SCALE: 1 IN = 1000 FT



WEST

PLATE #

TRASSER AL-YACOUB
 ER-3574

REPLACEMENT VELOCITY: 1.5000
 SURFACE VELOCITY: 1.5000
 SURFACE VELOCITY CENTER: 10000
 DATE: 10/20/67
 JOB: 9

RECORDING INFORMATION:

RECORDING SITE: 10000
 INSTRUMENT: 10000
 INSTRUMENT SERIAL: 10000
 INSTRUMENT TYPE: 10000
 INSTRUMENT MANUFACTURER: 10000
 INSTRUMENT MODEL: 10000
 INSTRUMENT SERIAL: 10000
 INSTRUMENT TYPE: 10000
 INSTRUMENT MANUFACTURER: 10000
 INSTRUMENT MODEL: 10000

Western Geophysical

PROCESSING INFORMATION:

1. FILTER: 10000
 2. GAIN: 10000
 3. SEGMENTATION: 10000
 4. SEGMENTATION: 10000
 5. SEGMENTATION: 10000
 6. SEGMENTATION: 10000
 7. SEGMENTATION: 10000
 8. SEGMENTATION: 10000
 9. SEGMENTATION: 10000
 10. SEGMENTATION: 10000

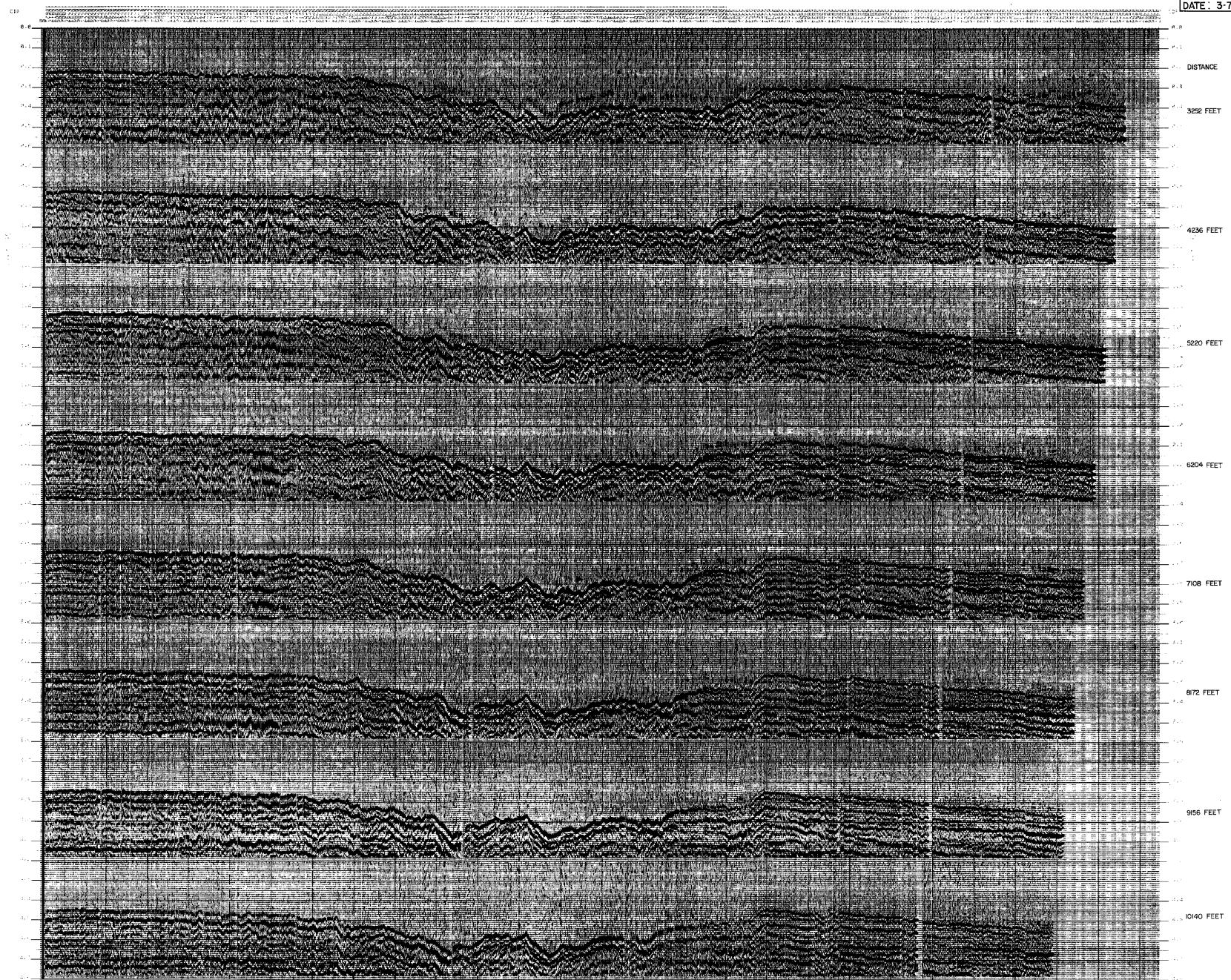
REMARKS:

1. SEGMENTATION: 10000
 2. SEGMENTATION: 10000
 3. SEGMENTATION: 10000
 4. SEGMENTATION: 10000
 5. SEGMENTATION: 10000
 6. SEGMENTATION: 10000
 7. SEGMENTATION: 10000
 8. SEGMENTATION: 10000
 9. SEGMENTATION: 10000
 10. SEGMENTATION: 10000



DETECTOR STATION NUMBER AXIS

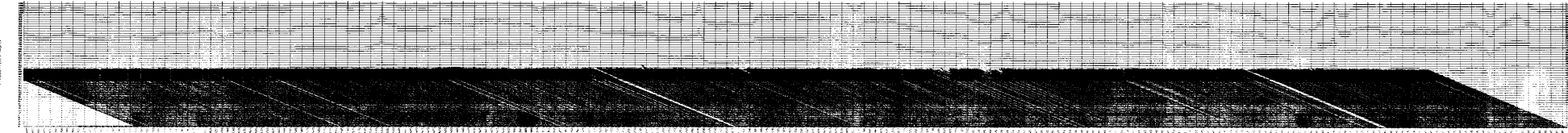
TAISSER AL-YACOUB
PLATE # 3
THESIS # ER-3574
DATE: 3-7-88



SDCT DISPLAY OF DETECTOR STATIONS NUMBER (HORIZONTAL AXIS) VERSUS SOURCE-TO-DETECTOR DISTANCE (VERTICAL AXIS) WITH A DIFFERENT OFFSET DISPLAY.

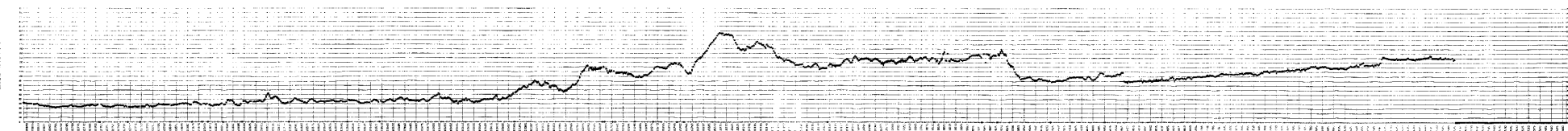
THOMAS AL. WOODS
P.O. BOX 200 (R.D. 1)
MOUNTAIN VIEW, TEXAS
DATE: 5-7-69

E. PLOT OF RECALCULATED PORE PRESSURE



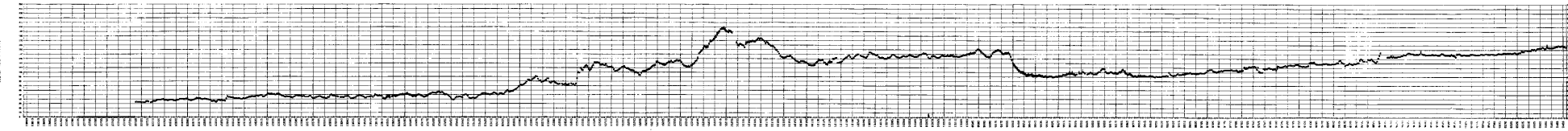
STATIONS

D. DEVIATION DEVIATION TIME DEVIATION DISTRIBUTION PLOT OF A LAYER



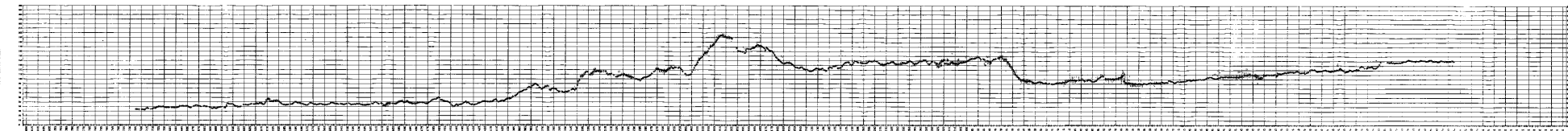
STATIONS

C. DEVIATION AND TIME DEVIATION DISTRIBUTION PLOT OF A LAYER



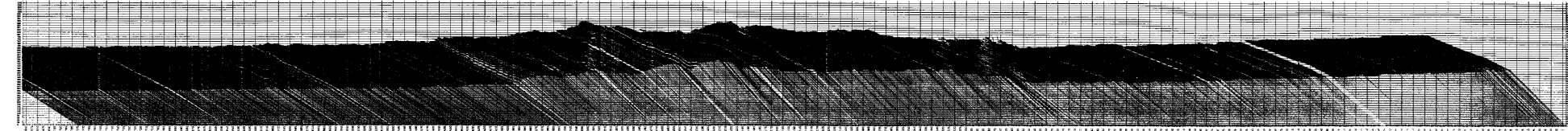
STATIONS

B. DEVIATION TIME DEVIATION DISTRIBUTION PLOT OF A LAYER



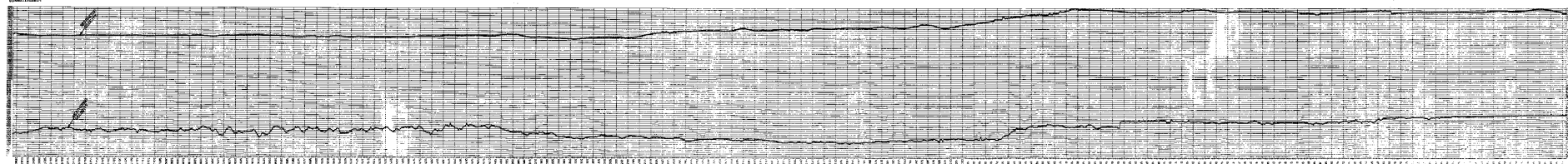
STATIONS

A. PLOT OF RECALCULATED ANNUAL PORE PRESSURE



1. POINT TO POINT

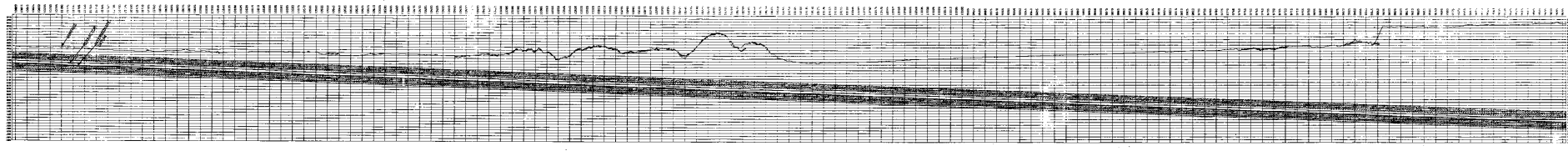
1000000



STATION 5

2. STATION TO STATION

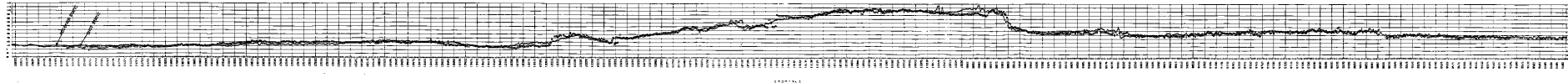
1000000



STATION 5

3. STATION TO STATION

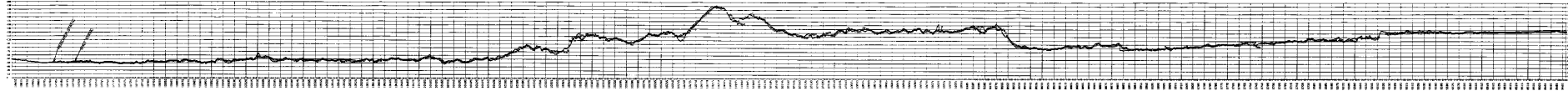
1000000



STATION 5

4. STATION TO STATION

1000000



STATION 5

PLATE 6
 VIB. PTS. 9477-10775
 REFRACTION BRUTE
 TRAISSER AL-YACOUB
 ER-3574

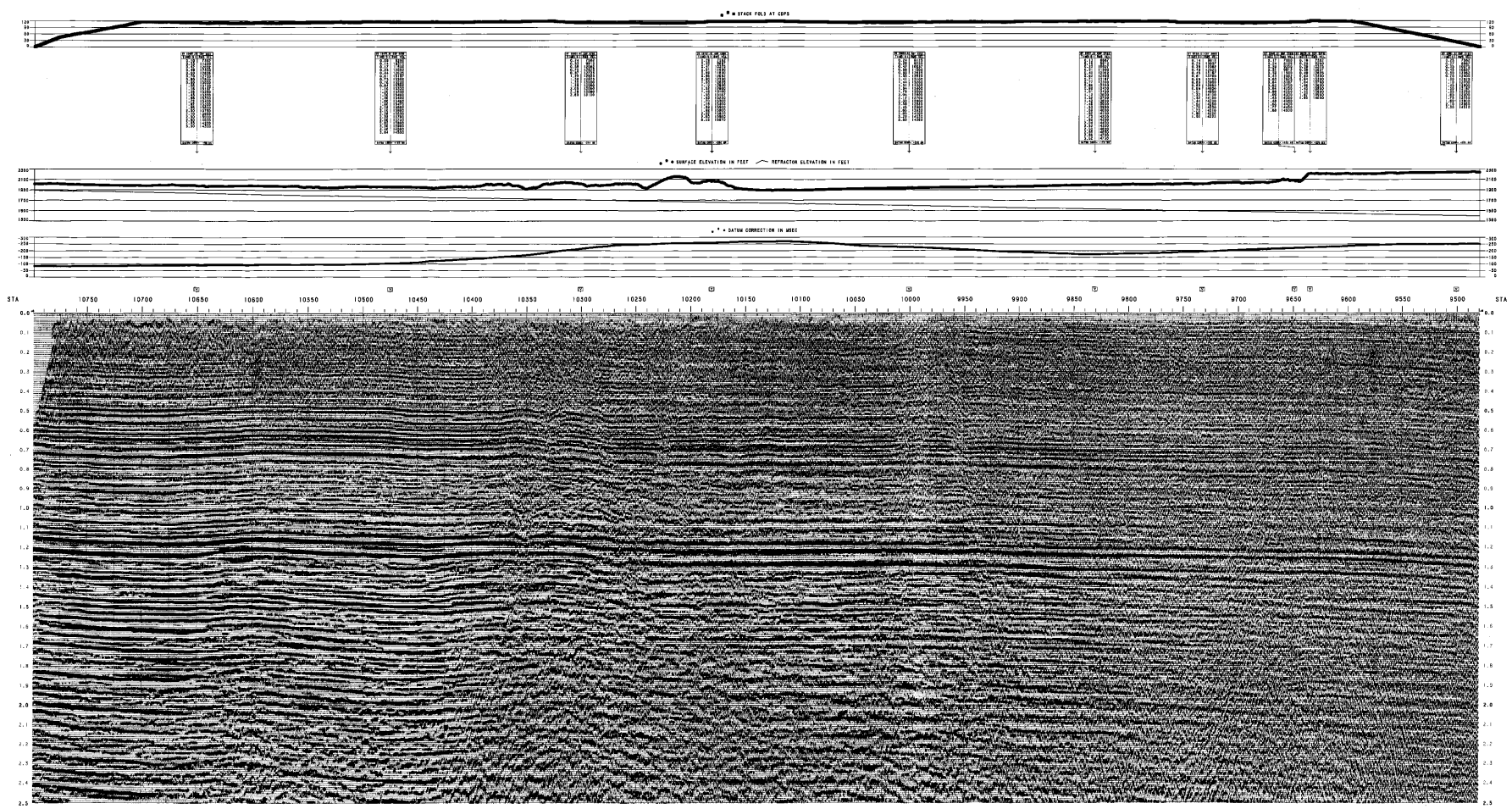


PLATE
 VIB. PTS. 9477-10775
 REFRACTION BRUTE

WEST

PLATE # 6

TRAISSER AL-YACOUB
ER-3574

INVESTIGATING AGENCY: **TRAISSER AL-YACOUB**
 DATE: **1988**
 PROJECT NO.: **ER-3574**
 SHEET NO.: **6**

RECORDING INFORMATION:

SEISMOLOGIST: **TRAISSER AL-YACOUB**

RECORDING METHOD: **VIBROSEISMIC**

RECORDING EQUIPMENT: **TRAISSER AL-YACOUB**

RECORDING SITE: **TRAISSER AL-YACOUB**

RECORDING DATE: **1988**

RECORDING TIME: **10:00 AM**

RECORDING LOCATION: **TRAISSER AL-YACOUB**

RECORDING INSTRUMENT: **TRAISSER AL-YACOUB**

RECORDING SENSITIVITY: **TRAISSER AL-YACOUB**

RECORDING GAIN: **TRAISSER AL-YACOUB**

RECORDING FILTERS: **TRAISSER AL-YACOUB**

RECORDING GEOPHYSICAL: **Western Geophysical**

PROCESSING SEQUENCE:

1. ANALOG TO DIGITAL CONVERSION
2. TIME CORRECTION AND STRETCHING
3. DECONVOLUTION
4. REFRACTION FILTERING
5. VELOCITY ANALYSIS
6. S-WAVE CORRECTION
7. S-WAVE SUPPRESSION
8. S-WAVE SUPPRESSION
9. S-WAVE SUPPRESSION
10. S-WAVE SUPPRESSION

REVISIONS:

REVISION NO. 1: **TRAISSER AL-YACOUB**

REVISION NO. 2: **TRAISSER AL-YACOUB**

REVISION NO. 3: **TRAISSER AL-YACOUB**

REVISION NO. 4: **TRAISSER AL-YACOUB**

REVISION NO. 5: **TRAISSER AL-YACOUB**

REVISION NO. 6: **TRAISSER AL-YACOUB**

REVISION NO. 7: **TRAISSER AL-YACOUB**

REVISION NO. 8: **TRAISSER AL-YACOUB**

REVISION NO. 9: **TRAISSER AL-YACOUB**

REVISION NO. 10: **TRAISSER AL-YACOUB**

REVISION NO. 11: **TRAISSER AL-YACOUB**

REVISION NO. 12: **TRAISSER AL-YACOUB**

REVISION NO. 13: **TRAISSER AL-YACOUB**

REVISION NO. 14: **TRAISSER AL-YACOUB**

REVISION NO. 15: **TRAISSER AL-YACOUB**

REVISION NO. 16: **TRAISSER AL-YACOUB**

REVISION NO. 17: **TRAISSER AL-YACOUB**

REVISION NO. 18: **TRAISSER AL-YACOUB**

REVISION NO. 19: **TRAISSER AL-YACOUB**

REVISION NO. 20: **TRAISSER AL-YACOUB**

REVISION NO. 21: **TRAISSER AL-YACOUB**

REVISION NO. 22: **TRAISSER AL-YACOUB**

REVISION NO. 23: **TRAISSER AL-YACOUB**

REVISION NO. 24: **TRAISSER AL-YACOUB**

REVISION NO. 25: **TRAISSER AL-YACOUB**

REVISION NO. 26: **TRAISSER AL-YACOUB**

REVISION NO. 27: **TRAISSER AL-YACOUB**

REVISION NO. 28: **TRAISSER AL-YACOUB**

REVISION NO. 29: **TRAISSER AL-YACOUB**

REVISION NO. 30: **TRAISSER AL-YACOUB**

REVISION NO. 31: **TRAISSER AL-YACOUB**

REVISION NO. 32: **TRAISSER AL-YACOUB**

REVISION NO. 33: **TRAISSER AL-YACOUB**

REVISION NO. 34: **TRAISSER AL-YACOUB**

REVISION NO. 35: **TRAISSER AL-YACOUB**

REVISION NO. 36: **TRAISSER AL-YACOUB**

REVISION NO. 37: **TRAISSER AL-YACOUB**

REVISION NO. 38: **TRAISSER AL-YACOUB**

REVISION NO. 39: **TRAISSER AL-YACOUB**

REVISION NO. 40: **TRAISSER AL-YACOUB**

REVISION NO. 41: **TRAISSER AL-YACOUB**

REVISION NO. 42: **TRAISSER AL-YACOUB**

REVISION NO. 43: **TRAISSER AL-YACOUB**

REVISION NO. 44: **TRAISSER AL-YACOUB**

REVISION NO. 45: **TRAISSER AL-YACOUB**

REVISION NO. 46: **TRAISSER AL-YACOUB**

REVISION NO. 47: **TRAISSER AL-YACOUB**

REVISION NO. 48: **TRAISSER AL-YACOUB**

REVISION NO. 49: **TRAISSER AL-YACOUB**

REVISION NO. 50: **TRAISSER AL-YACOUB**

REVISION NO. 51: **TRAISSER AL-YACOUB**

REVISION NO. 52: **TRAISSER AL-YACOUB**

REVISION NO. 53: **TRAISSER AL-YACOUB**

REVISION NO. 54: **TRAISSER AL-YACOUB**

REVISION NO. 55: **TRAISSER AL-YACOUB**

REVISION NO. 56: **TRAISSER AL-YACOUB**

REVISION NO. 57: **TRAISSER AL-YACOUB**

REVISION NO. 58: **TRAISSER AL-YACOUB**

REVISION NO. 59: **TRAISSER AL-YACOUB**

REVISION NO. 60: **TRAISSER AL-YACOUB**

REVISION NO. 61: **TRAISSER AL-YACOUB**

REVISION NO. 62: **TRAISSER AL-YACOUB**

REVISION NO. 63: **TRAISSER AL-YACOUB**

REVISION NO. 64: **TRAISSER AL-YACOUB**

REVISION NO. 65: **TRAISSER AL-YACOUB**

REVISION NO. 66: **TRAISSER AL-YACOUB**

REVISION NO. 67: **TRAISSER AL-YACOUB**

REVISION NO. 68: **TRAISSER AL-YACOUB**

REVISION NO. 69: **TRAISSER AL-YACOUB**

REVISION NO. 70: **TRAISSER AL-YACOUB**

REVISION NO. 71: **TRAISSER AL-YACOUB**

REVISION NO. 72: **TRAISSER AL-YACOUB**

REVISION NO. 73: **TRAISSER AL-YACOUB**

REVISION NO. 74: **TRAISSER AL-YACOUB**

REVISION NO. 75: **TRAISSER AL-YACOUB**

REVISION NO. 76: **TRAISSER AL-YACOUB**

REVISION NO. 77: **TRAISSER AL-YACOUB**

REVISION NO. 78: **TRAISSER AL-YACOUB**

REVISION NO. 79: **TRAISSER AL-YACOUB**

REVISION NO. 80: **TRAISSER AL-YACOUB**

REVISION NO. 81: **TRAISSER AL-YACOUB**

REVISION NO. 82: **TRAISSER AL-YACOUB**

REVISION NO. 83: **TRAISSER AL-YACOUB**

REVISION NO. 84: **TRAISSER AL-YACOUB**

REVISION NO. 85: **TRAISSER AL-YACOUB**

REVISION NO. 86: **TRAISSER AL-YACOUB**

REVISION NO. 87: **TRAISSER AL-YACOUB**

REVISION NO. 88: **TRAISSER AL-YACOUB**

REVISION NO. 89: **TRAISSER AL-YACOUB**

REVISION NO. 90: **TRAISSER AL-YACOUB**

REVISION NO. 91: **TRAISSER AL-YACOUB**

REVISION NO. 92: **TRAISSER AL-YACOUB**

REVISION NO. 93: **TRAISSER AL-YACOUB**

REVISION NO. 94: **TRAISSER AL-YACOUB**

REVISION NO. 95: **TRAISSER AL-YACOUB**

REVISION NO. 96: **TRAISSER AL-YACOUB**

REVISION NO. 97: **TRAISSER AL-YACOUB**

REVISION NO. 98: **TRAISSER AL-YACOUB**

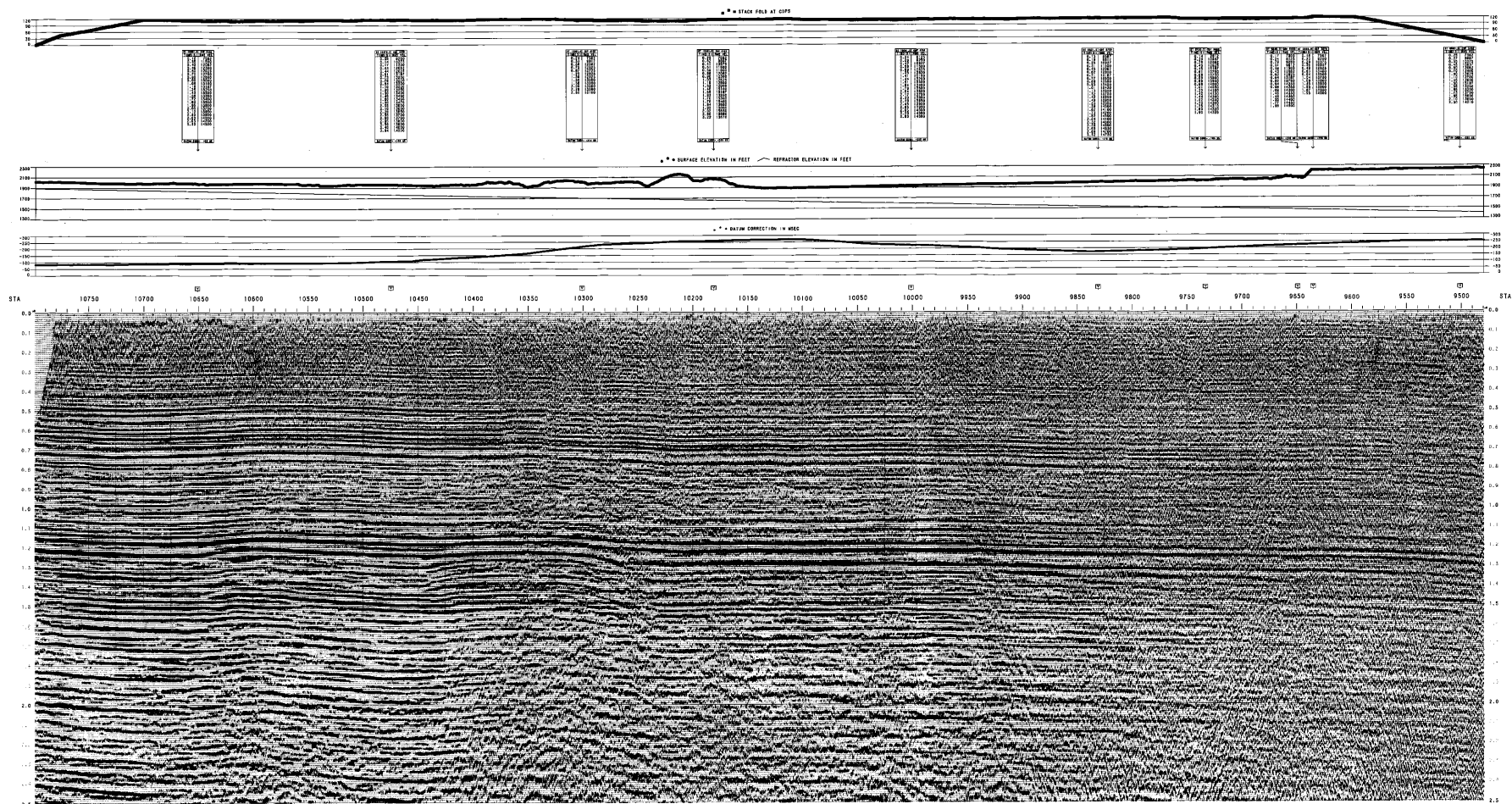
REVISION NO. 99: **TRAISSER AL-YACOUB**

REVISION NO. 100: **TRAISSER AL-YACOUB**



PLATE 7
 VIB. PTS. 9477-10775
 REFRACION MISER
 TRASSER AL-YACOUB
 ER-3574

PLATE 7
 VIB. PTS. 9477-10775
 REFRACION MISER



WEST

PLATE # 7

TRASSER AL-YACOUB
 ER-3574

RECORDING VELOCITY: 1800 FT/SEC
 RECORDING DATE: 1968
 REFRACION MISER
 WESTERN GEOLOGICAL CENTER

RECORDING INFORMATION:

RECORDING DATE: 1968
 RECORDING TIME: 10:00 AM
 RECORDING LOCATION: 10750-9500
 RECORDING METHOD: VIBROSEISMIC
 RECORDING SYSTEM: TRASSER AL-YACOUB
 RECORDING INSTRUMENT: TRASSER AL-YACOUB
 RECORDING GEOPHYSICIST: TRASSER AL-YACOUB

Western Geophysical

PROCESSING SCHEME:

1. INPUT DATA
2. PULSE CORRECTION
3. GROUND ROLL CORRECTION
4. VELOCITY CORRECTION
5. REFRACTIVE INDEX CORRECTION
6. NORMAL VELOCITY AND FIRST ORDER DISPERSION CORRECTION
7. STRETCH
8. FILTER

LABORATORY:

WESTERN GEOLOGICAL CENTER
 10750-9500

HORIZONTAL SCALE: 1 IN = 1000 FT
 VERTICAL SCALE: 1 IN = 100 MSEC